



**National Weather Service
National Centers
for
Environmental Prediction**

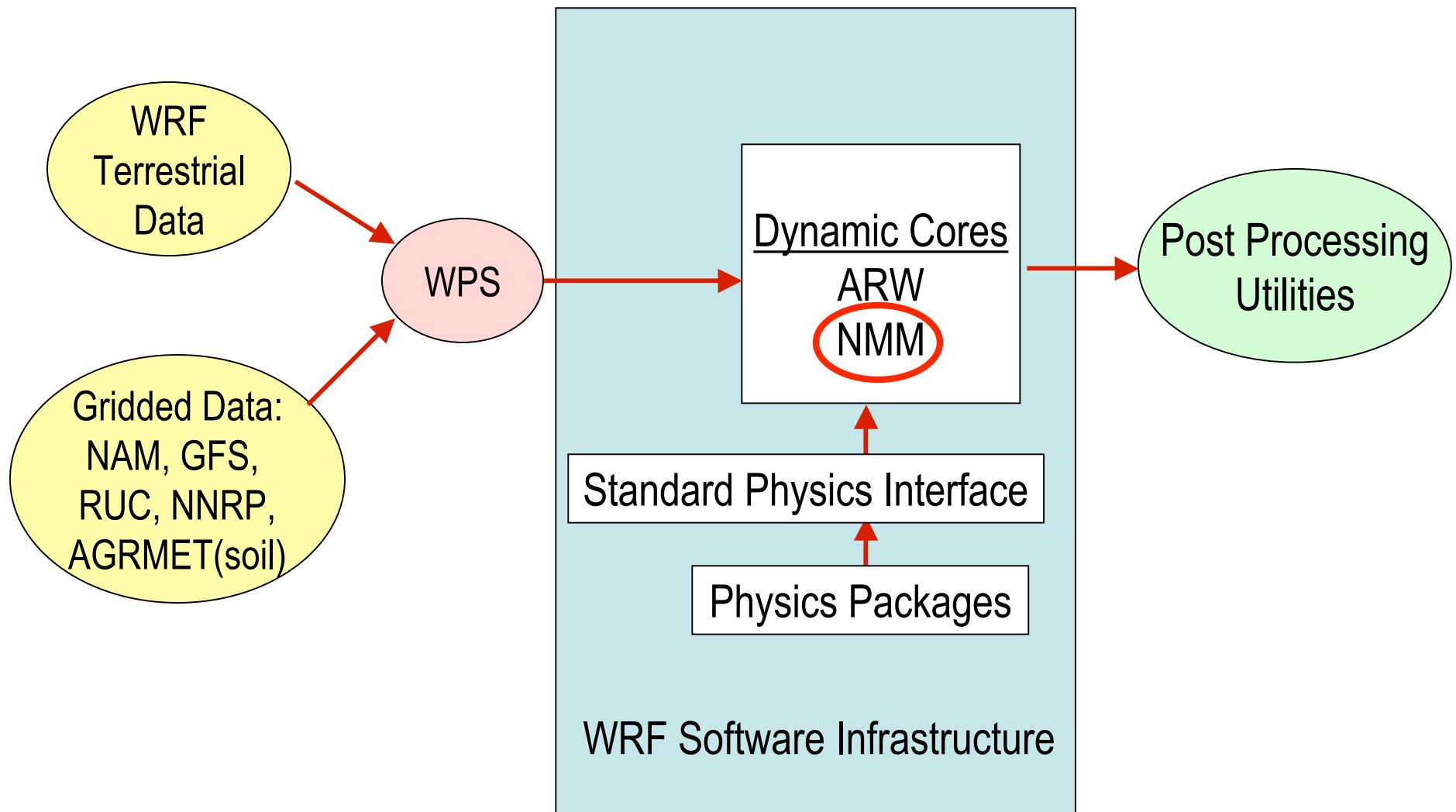


The WRF NMM Core

Overview of Basic Principles

Zavisa Janjic

WRF Modeling System



➤ OUTLINE

- Introduction
- Equations
- Boundary conditions
- Horizontal and vertical coordinates
- Basic discretization principles
- Horizontal grid
- Modeling nonlinear terms and basics of Fjortoft theory
- Horizontal nonlinear advection scheme for momentum
- General features of horizontal discrete operators
- Vertical grid
- Time stepping
- Passive substance advection
- Dissipation
- Examples
- Conclusions

➤ WRF-NMM built on experiences of NWP

- Relaxing the hydrostatic approximation, while,
- Using modeling principles proven in NWP and regional climate applications

➤ Nonhydrostatic equations split into two parts

- Hydrostatic part, except for higher order terms due to vertical acceleration
- The part that allows computation of the corrections in the first part

- No linearizations or additional approximations required, fully compressible system
- The nonhydrostatic effects as an add-on nonhydrostatic module
 - Easy comparison of hydrostatic and nonhydrostatic solutions
 - Reduced computational effort at lower resolutions

➤ Pressure based vertical coordinate.

- Exact mass (etc.) conservation
- Nondivergent flow on pressure surfaces (often forgotten)
- No problems with weak static stability

➤ Mass (hydrostatic pressure) based vertical coordinate

hydrostatic pressure = $\frac{\text{weight of the air in the column}}{\text{horizontal cross section of the column}}$

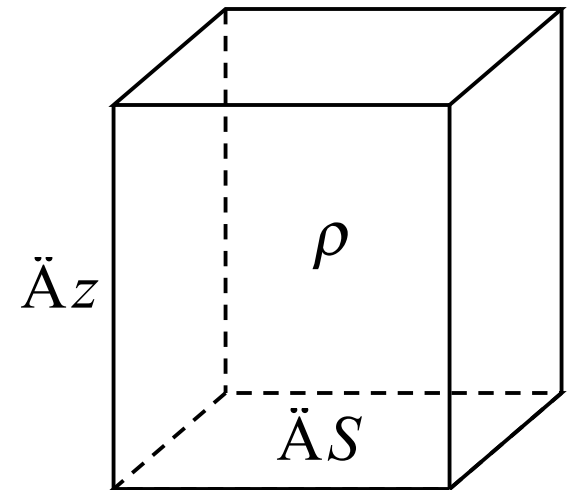
$$\rho = \frac{p}{RT}; \alpha = \frac{1}{\rho} = \frac{RT}{p}; p \text{ (nonhydrostatic) pressure}$$

$$\ddot{M} = \rho \ddot{S} \ddot{z}$$

$$\frac{g \ddot{M}}{\ddot{S}} = \rho g \ddot{z}$$

$$\ddot{\pi} = \rho \ddot{\Phi}; \pi \text{ hydrostatic pressure}$$

$$\frac{\ddot{\Phi}}{\ddot{\pi}} = \frac{1}{\rho} = \alpha$$



Hypsometric (**not hydrostatic**) equation

➤ Inviscid, adiabatic, sigma (Janjic et al., 2001):

$$\sigma = (\pi - \pi_t) / (\pi_s - \pi_t) \quad \mu = \pi_s - \pi_t \quad \varepsilon \equiv \frac{1}{g} \frac{dw}{dt}$$

$$\frac{d\mathbf{v}}{dt} = -(1 + \varepsilon) \nabla_\sigma \Phi - \alpha \nabla_\sigma p + f \mathbf{k} \times \mathbf{v}$$

$$\frac{\partial T}{\partial t} = -\mathbf{v} \cdot \nabla_\sigma T - \dot{\sigma} \frac{\partial T}{\partial \sigma} + \frac{\alpha}{c_p} \left[\frac{\partial p}{\partial t} + \mathbf{v} \cdot \nabla_\sigma p + \dot{\sigma} \frac{\partial p}{\partial \sigma} \right]$$

$$\frac{\partial \mu}{\partial t} + \nabla_\sigma \cdot (\mu \mathbf{v}) + \frac{\partial(\mu \dot{\sigma})}{\partial \sigma} = 0$$

Hydrostatic system,
except for p and ε

$$\alpha = RT / p$$

$$\frac{\partial \Phi}{\partial \sigma} = -\mu \frac{RT}{p}$$

$$\frac{\partial p}{\partial \pi} = 1 + \varepsilon \quad \text{3d Eq. of motion}$$

“Additional part”

$$\left(\frac{\partial T}{\partial t}\right)_2 = \frac{1}{c_p} \alpha \omega_2$$

$$\frac{\partial p}{\partial \pi} = 1 + \varepsilon \quad \text{Third (vertical) Eq of motion}$$

$$\frac{\partial \Phi}{\partial \sigma} = -\mu \frac{RT}{p}$$

$$w = \frac{1}{g} \frac{d\Phi}{dt} = \frac{1}{g} \left(\frac{\partial \Phi}{\partial t} + \mathbf{v} \cdot \nabla_{\sigma} \Phi + \sigma \frac{\partial \Phi}{\partial \sigma} \right) \quad \text{Nonhydrostatic cont. Eq}$$

$$\varepsilon = \frac{1}{g} \frac{dw}{dt} = \frac{1}{g} \left(\frac{\partial w}{\partial t} + \mathbf{v} \cdot \nabla_{\sigma} w + \sigma \frac{\partial w}{\partial \sigma} \right)$$

- Φ , w , ε not independent, no independent prognostic Eq for w !
- $\varepsilon \ll 1$ in meso and large scale atmospheric flows
- Impact of nonhydrostatic dynamics becomes detectable at resolutions $< 10\text{km}$, important at 1km .

➤ Boundary conditions

- $\dot{\sigma} = 0$ top
- $\dot{\sigma} = 0$ bottom

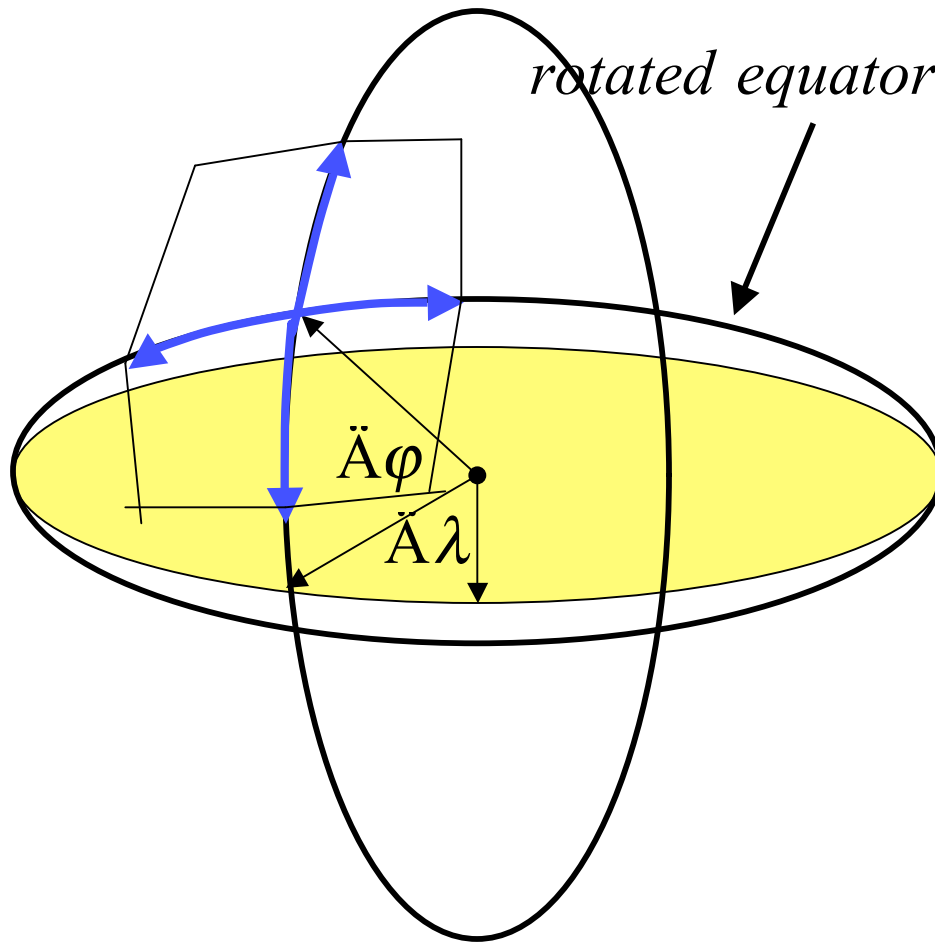
➤ Additional

- $p - \pi = 0$ top
- $\frac{\partial(p - \pi)}{\partial\sigma} = 0$ bottom

The rotated latitude-longitude projection

- Rotates the earth's latitude/longitude grid such that the intersection of the equator and prime meridian is at the center of the model domain.
- This rotation minimizes the convergence of meridians over the domain.
- Within the rotated framework the grid spacing is constant, but in an earth-relative sense the scale varies slightly.

➤ Rotated latitude-longitude coordinate



$$10^0 N < \varphi < 70^0 N$$

$$\Delta x \propto \cos(\varphi)$$

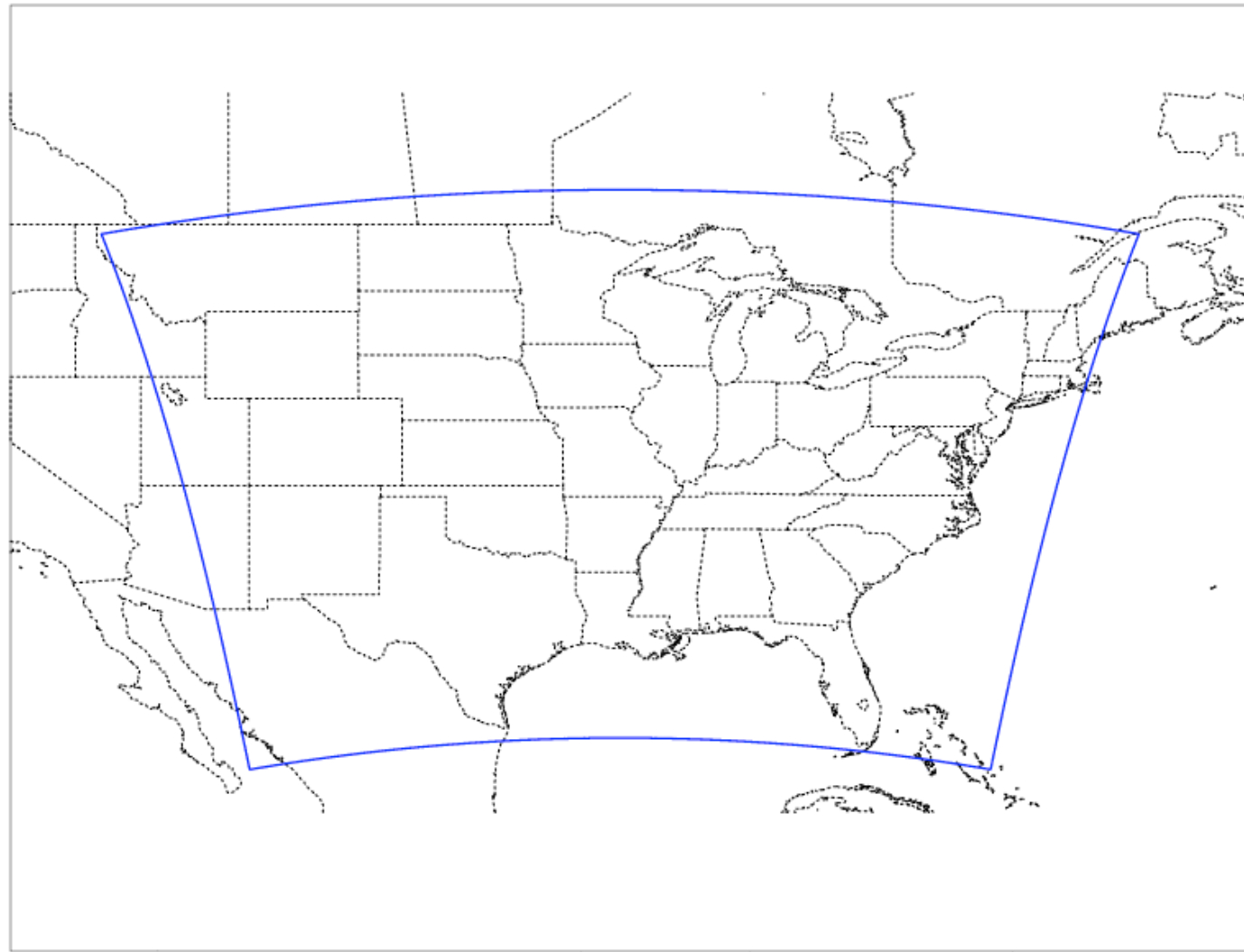
lat - lon

$$\cos(70^0) / \cos(10^0) = 0.3473$$

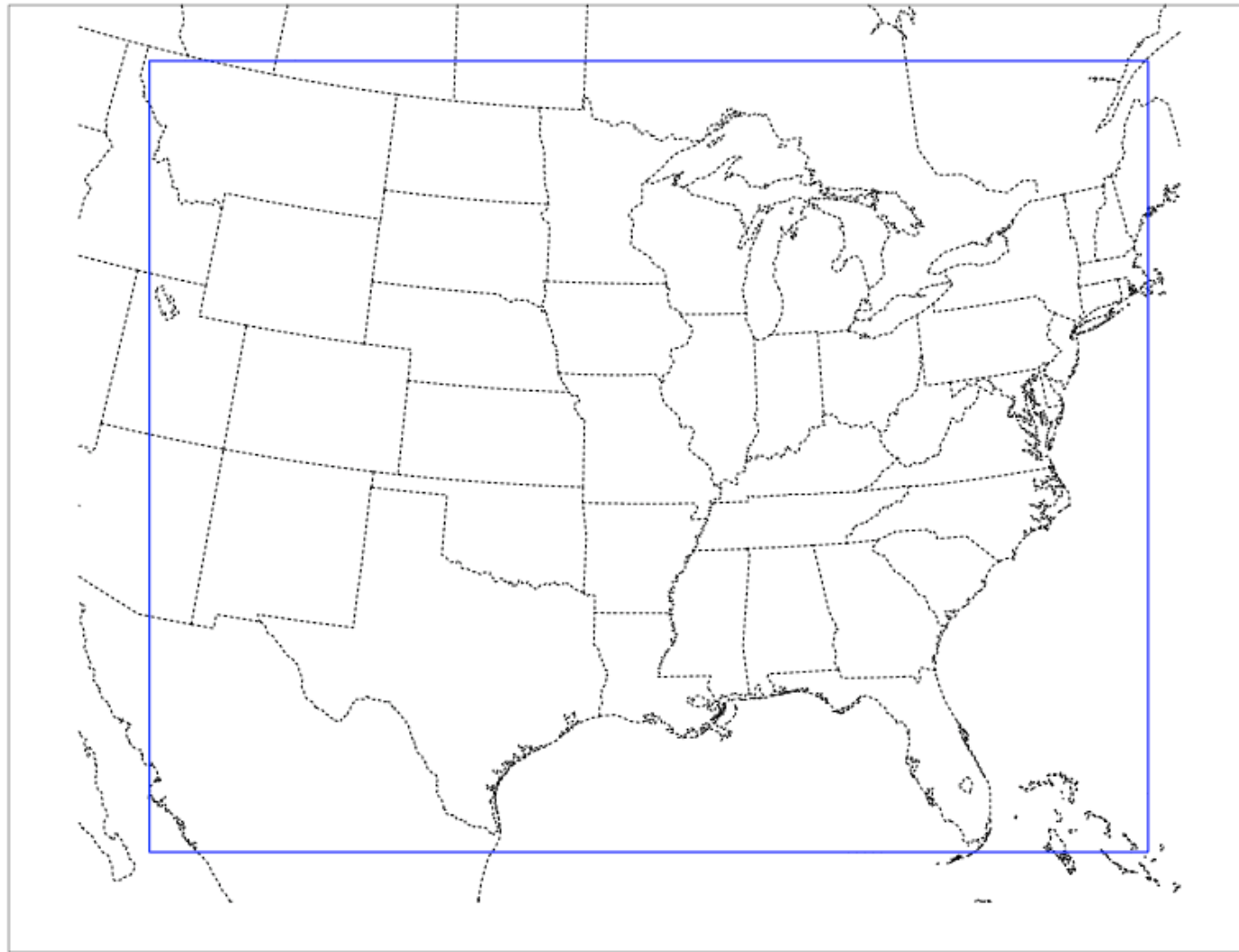
rotated lat - lon

$$\cos(30^0) / \cos(0^0) = 0.866$$

More uniform grid, longer time steps!



NMM rotlat domain (center 38N, 92W) projected on regular lat/lon map



Same domain projected on a similarly rotated lat/lon map background

```

subroutine tll(almd,aphd,tlm0d,ctph0,stph0,tlm,tph)
!
! *****
! *
! *   programmer: z. janjic, shmz, feb. 1981
! *   ammended:  z. janjic, ncep, jan. 1996
! *
! *   transformation from lat-lon to rotated lat-lon coordinates
! *****
!
! *   tlm   - transformed longitude, rad.
! *   tph   - transformed latitude, rad.
! *   tlm0d - the angle of rotation of the transformed lat-lon
! *           system in the longitudinal direction, degs
! *   ctph0 - cos(tph0), tph0 is the angle of rotation of the
! *           transformed lat-lon system in the latitudinal
! *           direction, precomputed
! *   stph0 - sin(tph0), tph0 is the angle of rotation of the
! *           transformed lat-lon system in the latitudinal
! *           direction, precomputed
! *   almd  - geographical longitude, degs, range -180.,180
! *   aphd  - geographical latitude,  degs, range - 90., 90.,
! *           poles are singular
! *****
!
parameter(dtr=3.1415926535897932384626433832795/180.)
!
relm=(almd-tlm0d)*dtr
srlm=sin(relm)
crlm=cos(relm)
aph=aphd*dtr
sph=sin(aph)
cph=cos(aph)
cc=cph*crlm
anum=cph*srlm
denom=ctph0*cc+stph0*sph
!
tlm=atan2(anum,denom)
arg=ctph0*sph-stph0*cc
if(arg.lt.-1.) arg=-1.
if(arg.gt. 1.) arg= 1.
tph=asin(arg)
!
return
end

```

$$\lambda' = \arctan \left[\frac{\cos(\varphi) \sin(\lambda - \lambda_0)}{\cos(\varphi_0) \cos(\varphi) \cos(\lambda - \lambda_0) + \sin(\varphi_0) \sin(\varphi)} \right]$$

$$\varphi' = \arcsin [\cos(\varphi_0) \sin(\varphi) - \sin(\varphi_0) \cos(\varphi) \cos(\lambda - \lambda_0)]$$

```

subroutine rtll(tlm,tph,tlm0d,ctph0,stph0,almd,aphd)
!
! *****
! *
! * programmer: z. janjic, shmz, feb. 1981
! * ammended: z. janjic, ncep, jan. 1996
! *
! * transformation from rotated lat-lon to lat-lon coordinates
! *****
!
! * tlm - transformed longitude, rad.
! * tph - transformed latitude, rad.
! * tlm0d - the angle of rotation of the transformed lat-lon
! * system in the longitudinal direction, degs
! * ctph0 - cos(tph0), tph0 is the angle of rotation of the
! * transformed lat-lon system in the latitudinal
! * direction, precomputed
! * stph0 - sin(tph0), tph0 is the angle of rotation of the
! * transformed lat-lon system in the latitudinal
! * direction, precomputed
! * almd - geographical longitude, degs, range -180.,180
! * aphd - geographical latitude, degs, range - 90., 90.,
! * poles are singular
! *****
!
parameter(dtr=3.1415926535897932384626433832795/180.)
!
stlm=sin(tlm)
ctlm=cos(tlm)
stph=sin(tph)
ctph=cos(tph)
!
sph=ctph0*stph+stph0*ctph*ctlm
sph=min(sph,1.)
sph=max(sph,-1.)
aph=asin(sph)
aphd=aph/dtr
anum=ctph*stlm
denom=(ctlm*ctph-stph0*sph)/ctph0
relm=atan2(anum,denom)
almd=relm/dtr+tlm0d
!
if(almd.gt. 180.) almd=almd-360.
if(almd.lt.-180.) almd=almd+360.
!
return
end

```

$$\varphi = \arcsin[\cos(\varphi_0) \sin(\varphi') + \sin(\varphi_0) \cos(\varphi') \cos(\lambda')]$$

$$\lambda = \arctan \left[\frac{\cos(\varphi') \sin(\lambda')}{\cos(\varphi') \cos(\lambda') - \sin(\varphi_0) \sin(\varphi)} \right] + \lambda_0$$

Velocity components must be rotated as well!

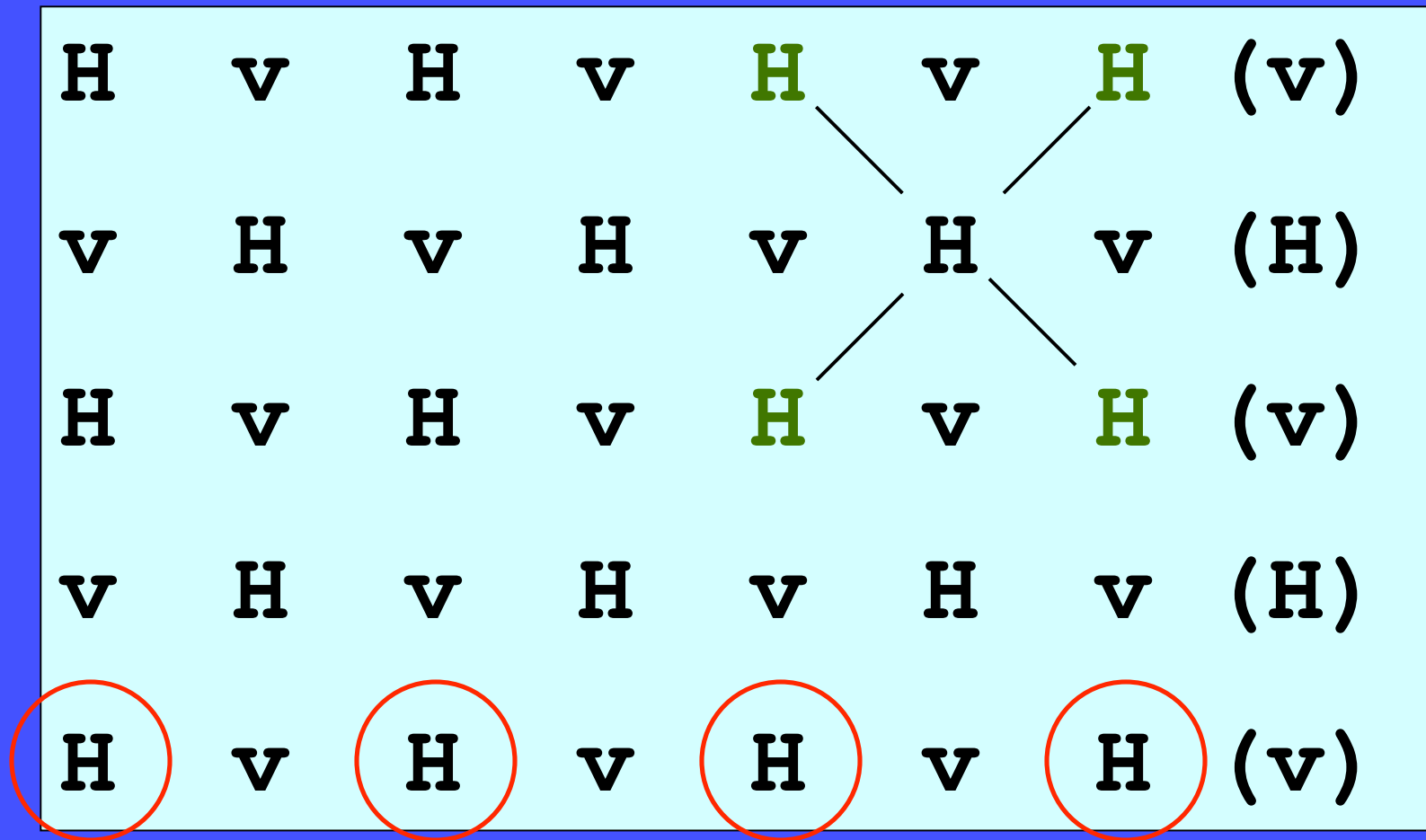
The E-grid stagger

H	v	H	v	H	v	H	(v)
v	H	v	H	v	H	v	(H)
H	v	H	v	H	v	H	(v)
<u>v</u>	<u>H</u>	v	H	v	H	v	(H)
H	v	H	v	H	v	H	(v)

H=mass point, v=wind point

red=(1,1) ; blue=(1,2)

The E-grid stagger



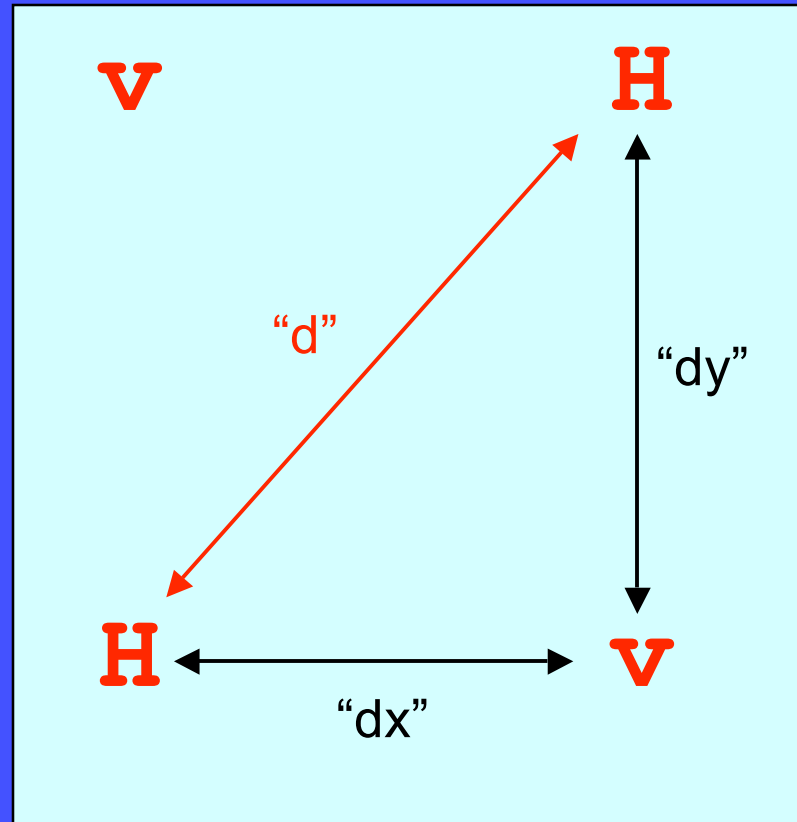
XDIM=4 (# of mass points on odd numbered row)

YDIM=5 (number of rows)

The E-grid stagger

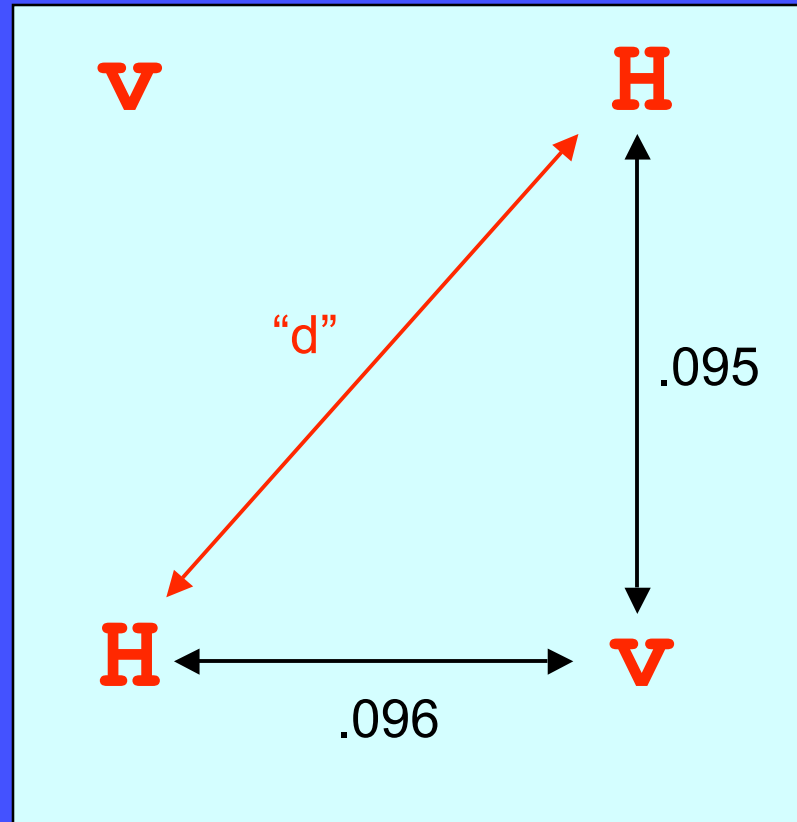
- Due to the indexing convention, the X-dimension is half as large as would be expected from a C-grid domain (XDIM typically quite a bit smaller than YDIM for the E-grid).
- “Think diagonally” – finite differences frequently are computed along the shortest distance between adjacent points, which is along the diagonals of the grid.

The E-grid stagger (cont.)



- conventional grid spacing "d" is the diagonal distance between two mass variable (H) points.
- grid spacing in the WPS namelist are the "dx" and "dy" values, specified in fractions of a degree.

The E-grid stagger (cont.)

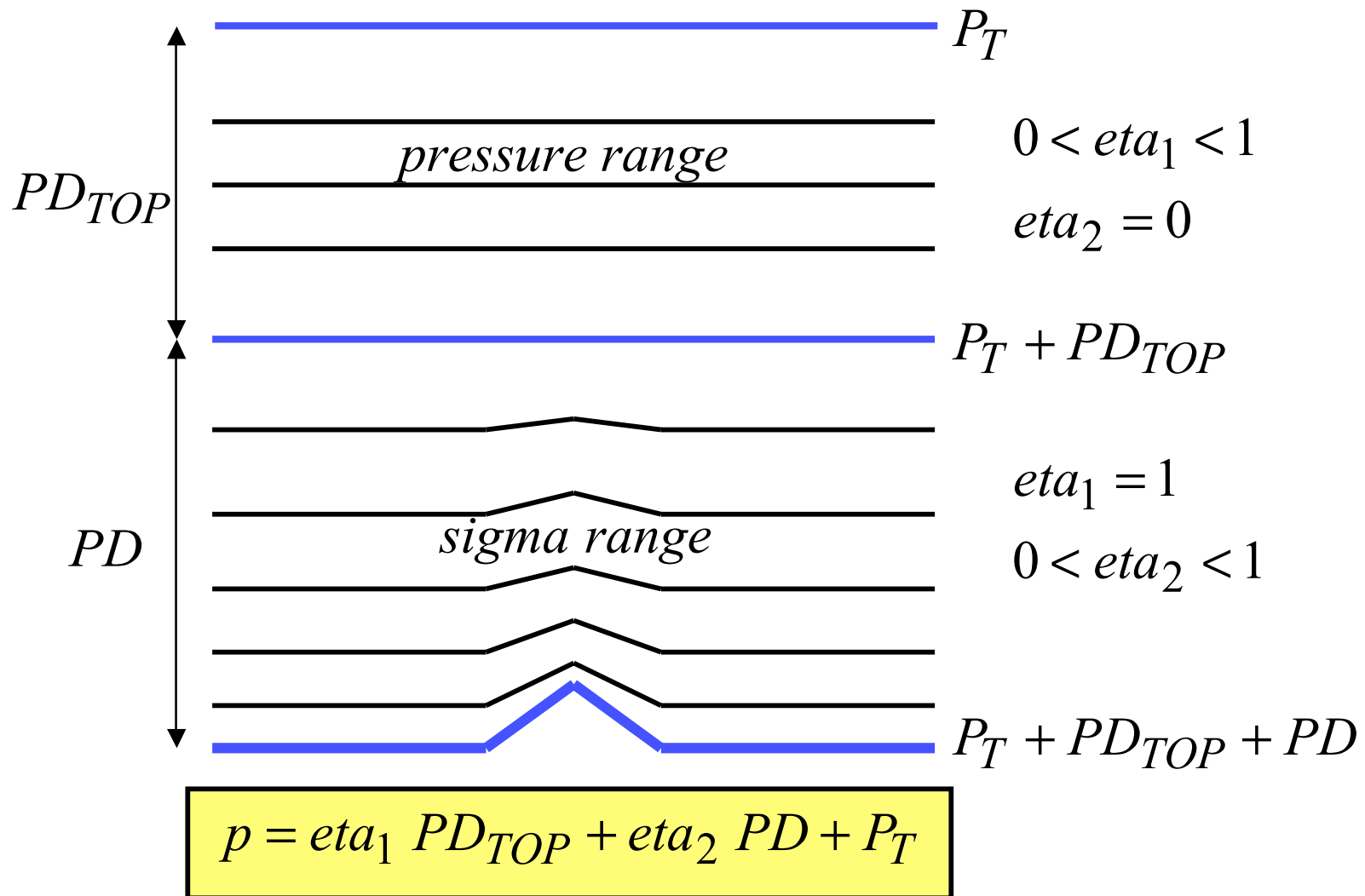


- $d \approx \sqrt{0.096^2 + 0.095^2} * (111.2 \text{ km/deg}) \approx 15 \text{ km}$
- The “WRF domain wizard” takes input grid spacing in km and computes the angular distances for the namelist.

➤ Pressure-sigma hybrid (Arakawa and Lamb, 1977).

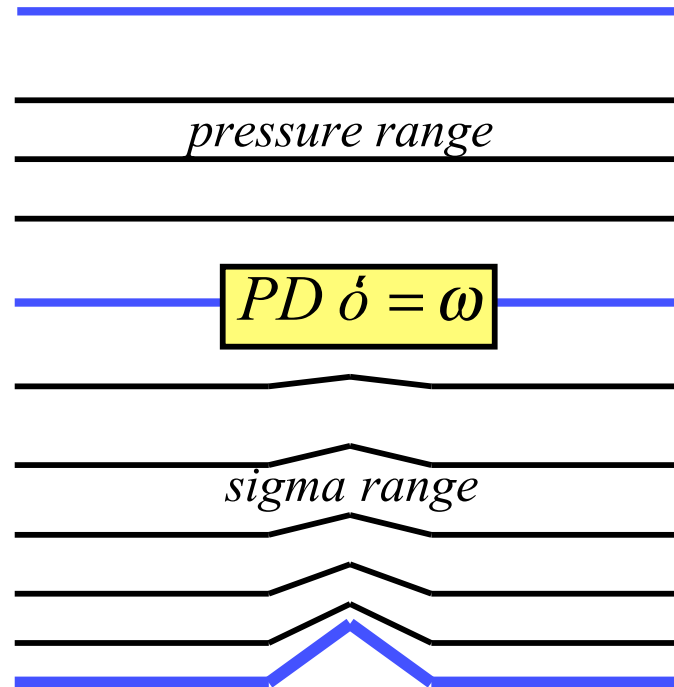
- Flat coordinate surfaces at high altitudes where sigma problems worst (e.g. Simmons and Burridge, 1981)
- Higher vertical resolution over elevated terrain
- No discontinuities and internal boundary conditions

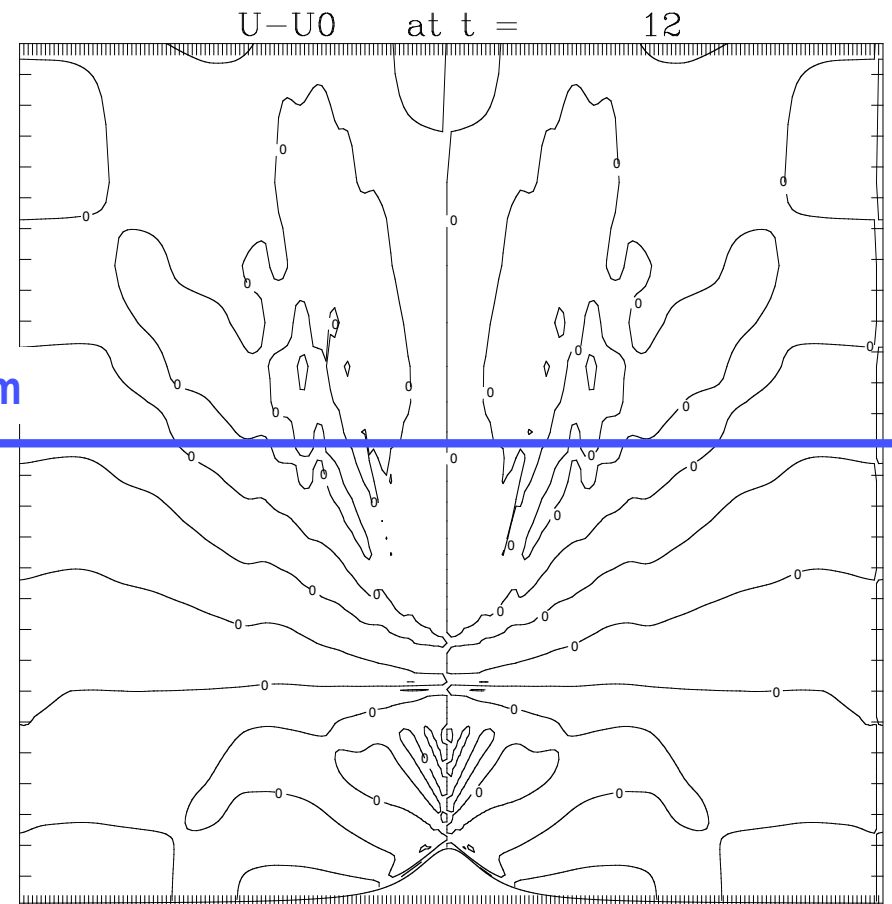
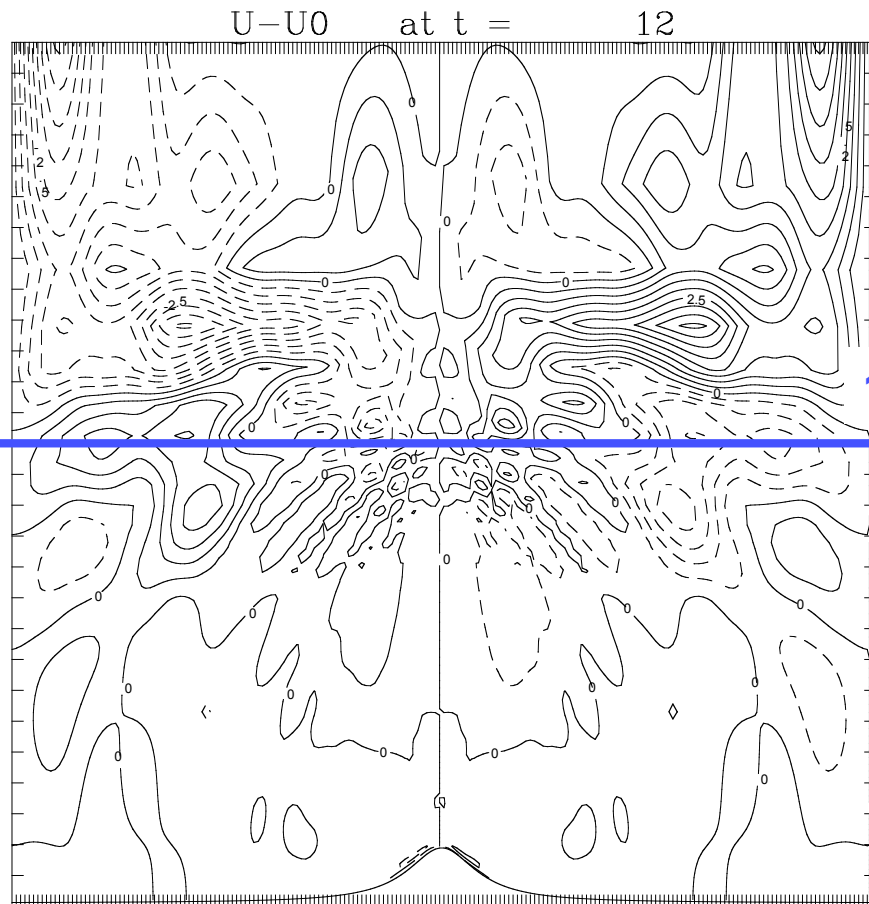
➤ Hybrid vertical coordinate



➤ Equations in hybrid coordinate

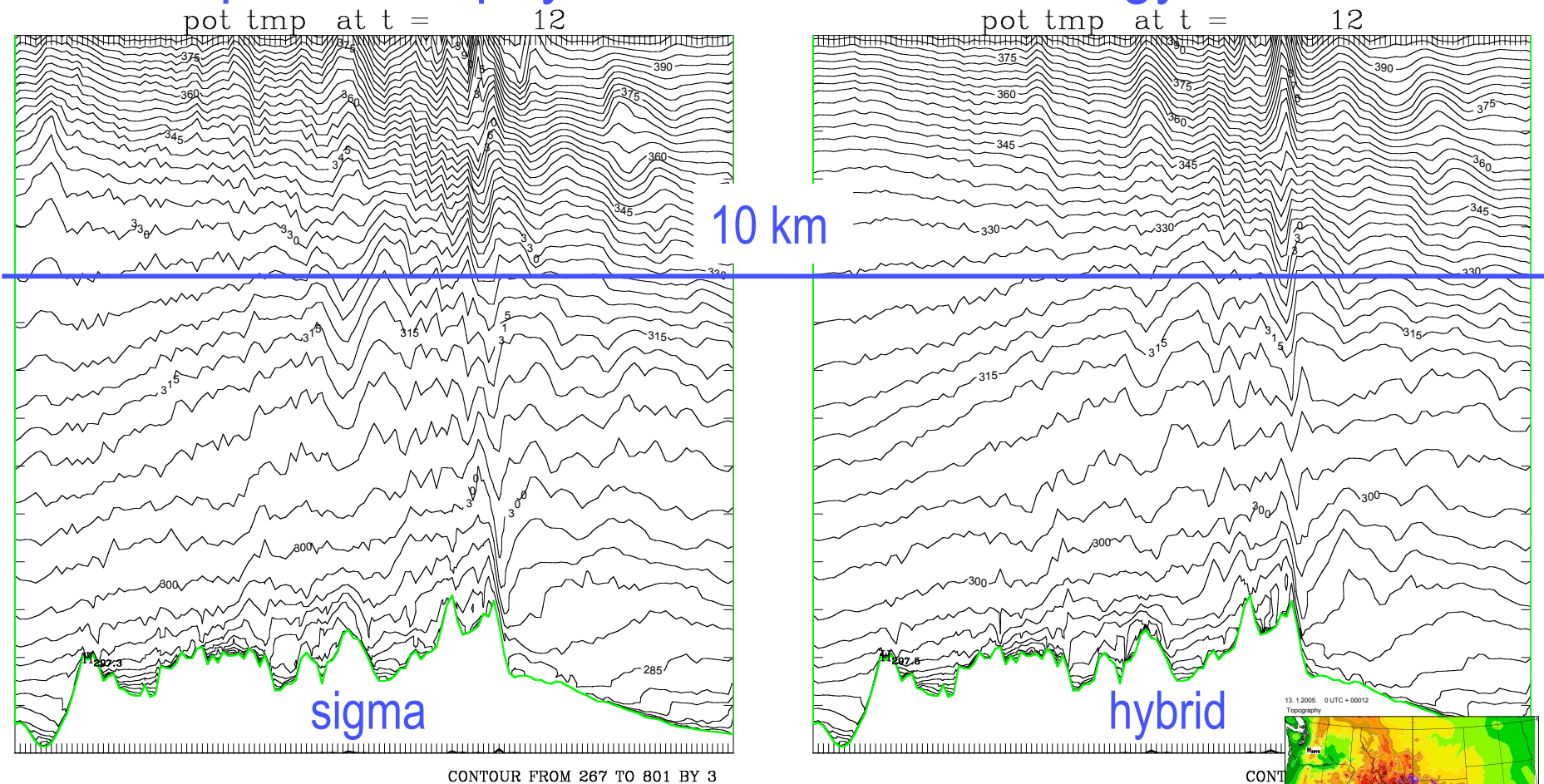
$$\frac{\partial PD}{\partial t} + \nabla_{\sigma} \cdot (PD \mathbf{v}) + \frac{\partial(PD \sigma')}{\partial \sigma} = 0$$
$$\nabla_p \cdot (\mathbf{v}) + \frac{\partial \omega}{\partial p} = 0$$



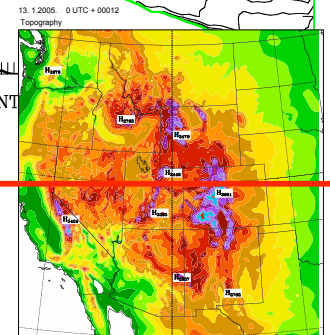


Wind component developing due to the spurious pressure gradient force in the sigma coordinate (left panel), and in the hybrid coordinate with the boundary between the pressure and sigma domains at about 400 hPa (right panel). Dashed lines represent negative values.

Example of nonphysical small scale energy source



Potential temperature, January 13, 2005, 00Z
12 hour forecasts, 3 deg contours



➤ Basic discretization principle is conservation of important properties of the continuous system.

- “Mimetic” approach

<http://www.math.unm.edu/~stanly/mimetic.html>

- Major novelty in applied mathematics, ...
- ... but well established in atmospheric modeling
(Arakawa, 1966, 1972, 1977 ...; Sadourny, 1975 ...; Janjic, 1977, 1984 ...; Tripoli, 1992, ...)

➤ Criteria chosen

- Energy and enstrophy conservation in order to control nonlinear energy cascade
- A number of first order and quadratic quantities conserved
- A number of properties of differential operators preserved
- Omega-alpha term, consistent transformations between KE and PE
- Minimized errors due to representation of orography

➤ Arakawa criteria for choosing grid, large scales:

- Geostrophic adjustment
- External and internal gravity-inertia wave frequencies on rectangular grids with 2nd order finite differencing (Winninghoff 1968; Arakawa and Lamb 1977, MCP; Janjic 1984, MWR; Randall, 1994, MWR; Gavrilov, 2004, MWR), classical synoptic scale design

<i>h</i>		<i>h</i>		<i>h</i>
	v		v	
<i>h</i>		<i>h</i>		<i>h</i>
	v		v	
<i>h</i>		<i>h</i>		<i>h</i>

B

<i>h</i>	<i>u</i>	<i>h</i>	<i>u</i>	<i>h</i>
<i>v</i>		<i>v</i>		<i>v</i>
<i>h</i>	<i>u</i>	<i>h</i>	<i>u</i>	<i>h</i>
<i>v</i>		<i>v</i>		<i>v</i>
<i>h</i>	<i>u</i>	<i>h</i>	<i>u</i>	<i>h</i>

C

<i>h</i>	v	<i>h</i>	v
v	<i>h</i>	v	<i>h</i>
<i>h</i>	v	<i>h</i>	v
v	<i>h</i>	v	<i>h</i>

E

<i>h,χ,ψ</i>	<i>h,χ,ψ</i>	<i>h,χ,ψ</i>
<i>h,χ,ψ</i>	<i>h,χ,ψ</i>	<i>h,χ,ψ</i>
<i>h,χ,ψ</i>	<i>h,χ,ψ</i>	<i>h,χ,ψ</i>

B'/Z

Janjic 1984; Randall 1994;
Gavrilov 2004, MWR

➤ Problems due to averaging

- C grid problems in the **entire admissible wavenumber range** with group velocity of (mostly internal) gravity-inertia waves in case of coarse resolution or **weak static stability** due to averaging of Coriolis force
- B/E grid problems with **small-scale** low-frequency noise due to averaging of divergence component terms
- **Advantage B/E grid**
- E grid initial formulation (ESMF compliant unified B grid model also under development)

➤ Nonlinear terms

- Due to nonlinearity, numerical models generally generate excessive small scale noise
- A major noise source is false nonlinear energy cascade (Phillips, 1954; Arakawa, 1966 ... ; Sadourny, 1975; ...)
- Accumulation of energy at small scales, distortion of spectrum and nonlinear instability

➤ Other computational errors as noise sources (e.g. sigma coordinate)

➤ Historically, the problem controlled by:

- Removing spurious small scale energy by filtering, dissipation
- Preventing excessive noise generation by enstrophy and energy conservation (Arakawa, 1966 ...)

Classical paper by Sadourny, 1975, JAS:

the “inertial” range; however, a correct energy spectrum for a numerical solution is not by itself a proof of the accuracy of the simulated energy transfers. In fact, it is always possible to force the energy distribution of any numerical solution to conform to a known spectral shape in the inertial range through ad-hoc assumptions, regarding, for instance, addition of artificial viscosity. However, if we are to trust numerical modeling as a method for providing better understanding of the real processes, we must then admit that a realistic energy spectrum should not be forced by artificial techniques, but should come instead as a by-product of the

first principles only, via correct treatment of the non-linear interactions. More precisely, accurate long-term statistical distributions of kinetic energy should result from:

1) An accurate distribution of sources and sinks (outside the inertial range).

2) Accurate representation of the statistical transfers of energy within the resolved scales (“internal” transfers) in spite of the truncation error of the finite-difference scheme in the smaller scales.

3) An accurate parameterization of the statistical effects of nonlinear interactions with the subgrid-scale motions.

➤ It is important that the statistical properties of the spectrum be obtained in a physically correct way!

- Barotropic nondivergent vorticity Eq., Charney, Fjortoft & von Neumann started NWP from

$$\frac{\partial \zeta}{\partial t} + J(\psi, \zeta) = 0, \quad \zeta = \nabla^2 \psi$$

- Essence of large scale atmospheric flow regime

$$\overline{\psi \frac{\partial \zeta}{\partial t}} = -\overline{\psi J(\psi, \zeta)} = 0$$

$$\overline{\zeta \frac{\partial \zeta}{\partial t}} = -\overline{\zeta J(\psi, \zeta)} = 0$$

$$\overline{K} = \frac{1}{2} \overline{(\nabla \psi)^2} = \text{const}, \quad \overline{\eta} = \frac{1}{2} \overline{(\nabla^2 \psi)^2} = \text{const}$$

ψ_n orthogonal functions, Parseval theorem,

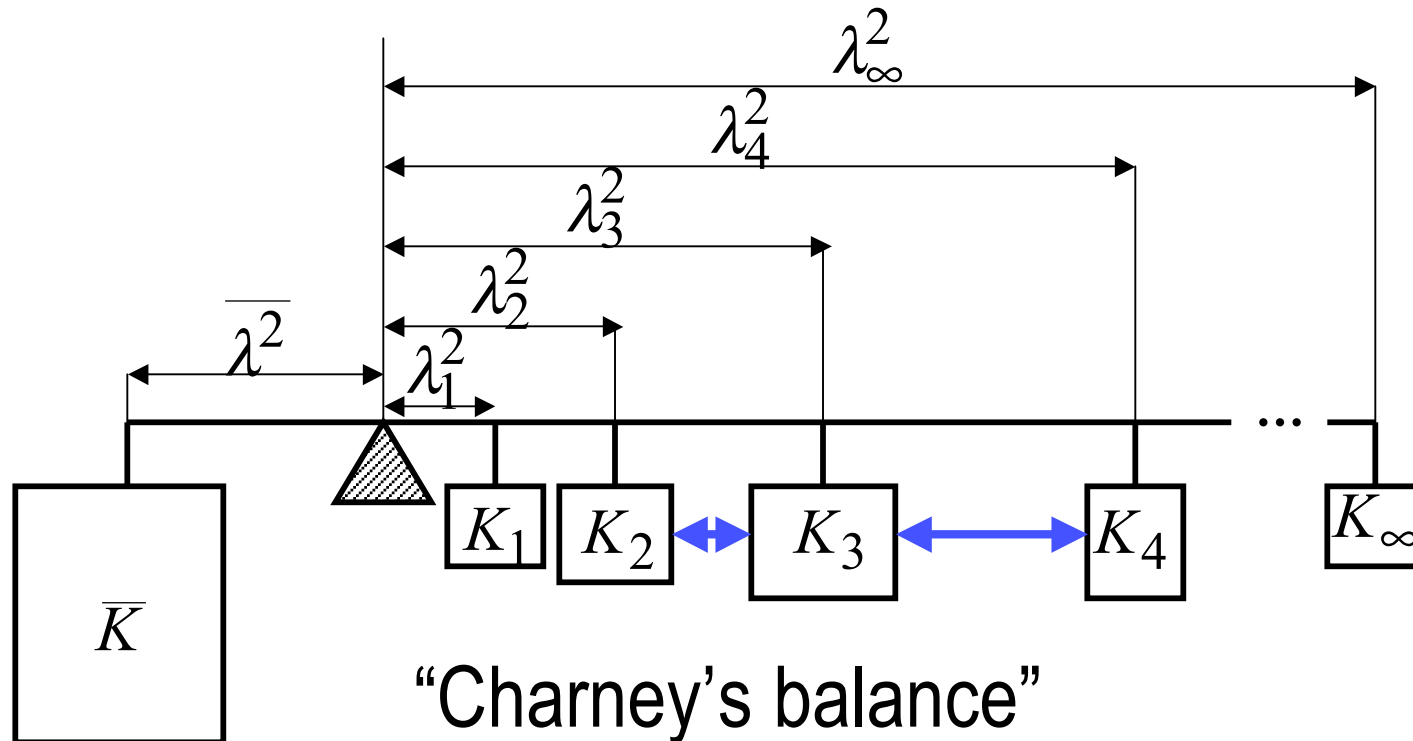
$$\overline{K} = \frac{1}{2} \sum_n \lambda_n^2 \psi_n^2 = \text{const}, \quad \overline{\eta} = \frac{1}{2} \sum_n \lambda_n^4 \psi_n^2 = \text{const}$$

Eigenvalues of Laplacian

$$\overline{K} = \frac{1}{2} \sum_n K_n = \text{const}, \quad \overline{\eta} = \frac{1}{2} \sum_n \lambda_n^2 K_n = \text{const}$$

$$\overline{\lambda^2} = \frac{\overline{\eta}}{\overline{K}} = \frac{\sum_n \lambda_n^2 K_n}{\sum_n K_n} = \text{const}$$

$$\boxed{\overline{\lambda^2}} \overline{K} = \sum_n \boxed{\lambda_n^2} K_n$$



$$\Delta K_1 + \Delta K_2 + \Delta K_3 = 0$$

$$\lambda_1^2 \Delta K_1 + \lambda_2^2 \Delta K_2 + \lambda_3^2 \Delta K_3 = 0$$

$$\lambda_1^2 < \lambda_2^2 < \lambda_3^2$$

$$\Delta K_1 = -\frac{(\lambda_3^2 - \lambda_2^2)}{(\lambda_3^2 - \lambda_1^2)} \Delta K_2$$

$$\Delta K_3 = -\frac{(\lambda_2^2 - \lambda_1^2)}{(\lambda_3^2 - \lambda_1^2)} \Delta K_2$$

- Triads, Fjortoft's theorem
- Downscale energy cascade restricted!
- Fundamental property of the fluid!

➤ Very interesting possibilities on the E grid

Nonlinear Advection Schemes and Energy Cascade on Semi-Staggered Grids

ZAVIŠA I. JANJIĆ

Federal Hydrometeorological Institute, Belgrade, Yugoslavia

(Manuscript received 4 October 1982, in final form 29 February 1984)

ABSTRACT

A common problem with nonlinear advection schemes is the false accumulation of energy at the smallest resolvable scales. To keep this process under control, following Arakawa (1966), a number of energy and enstrophy conserving schemes for staggered and semi-staggered grids have been designed. In this paper, it is demonstrated that, in contrast to the staggered grid, the conservation of energy and enstrophy on the semi-staggered grids does not guarantee that the erroneous transport of energy from large to small scales will be effectively restricted.

Using a new approach to the application of the Arakawa Jacobian, a scheme for a semi-staggered grid which exactly reflects the Arakawa theory for nondivergent flow is obtained for the first time. This is achieved by conservation of energy and enstrophy as defined on the staggered grid. These two quantities are of higher accuracy and cannot be calculated directly from the dependent variables on the semi-staggered grid. It is further demonstrated that the amount of energy which can be transported toward smaller scales is more restricted than for any other scheme of this type on both staggered and semi-staggered grids.

Experiments performed with the proposed scheme and a scheme which conserves energy and enstrophy as defined on the semi-staggered grid reveal visible differences in long-term integrations which are in agreement with the theory and demonstrate the advantages of the new scheme.

Retyped from the red box on the previous slide for better visibility:

“Using a new approach to the application of the Arakawa Jacobian, a scheme for a semi-staggered grid which exactly reflects the Arakawa theory is obtained for the first time. This is achieved by conservation of energy and enstrophy as defined on the staggered grid. These two quantities are of higher accuracy and cannot be calculated directly from the dependent variables on the semi-staggered grid. It is further demonstrated that the amount of energy which can be transported toward smaller scales is more restricted than for any other scheme of this type on both staggered and semi-staggered grids.”

Distances of weights on Charney balance with Janjic (1984) scheme

Definite advantage of E(B) grid over the C grid!

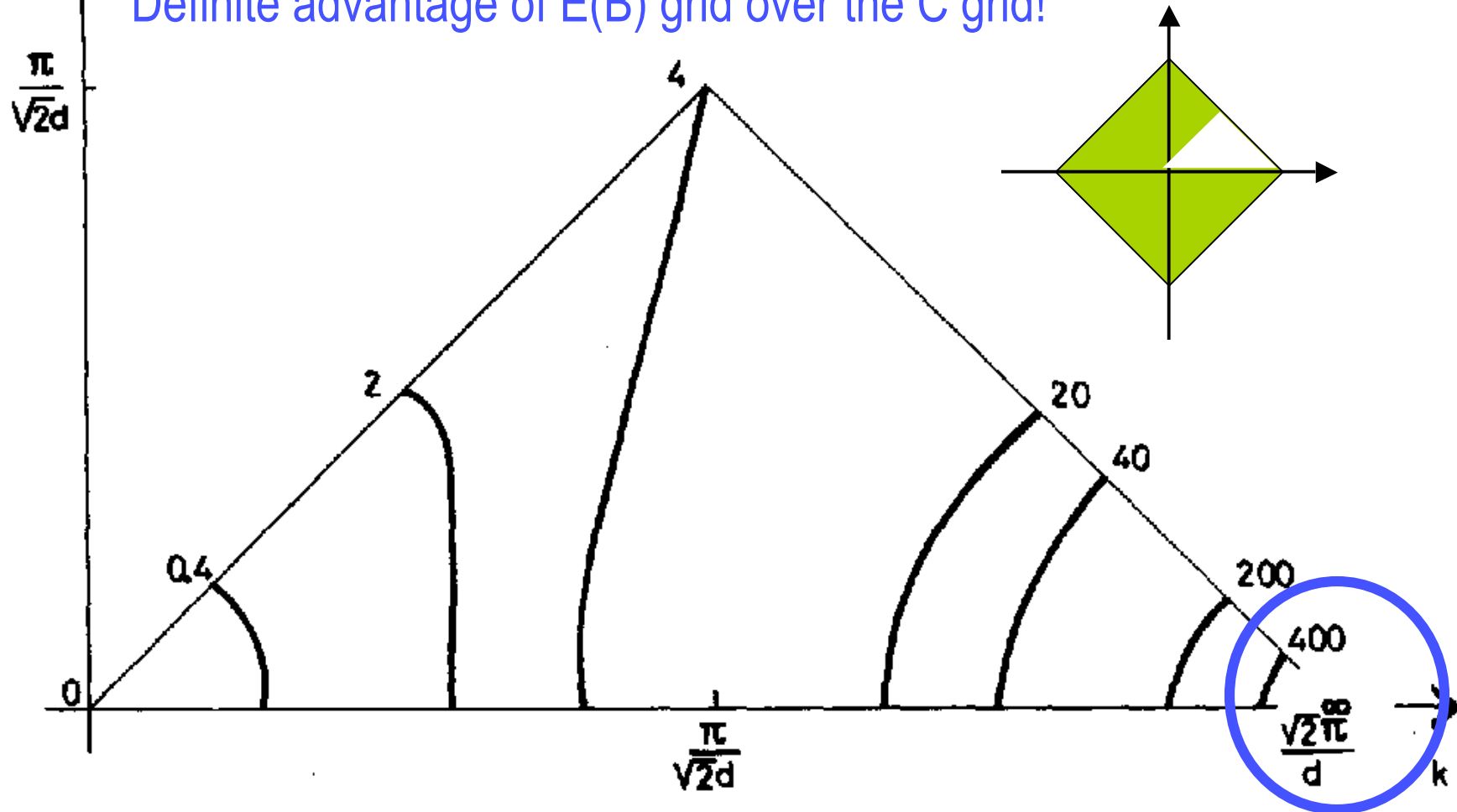
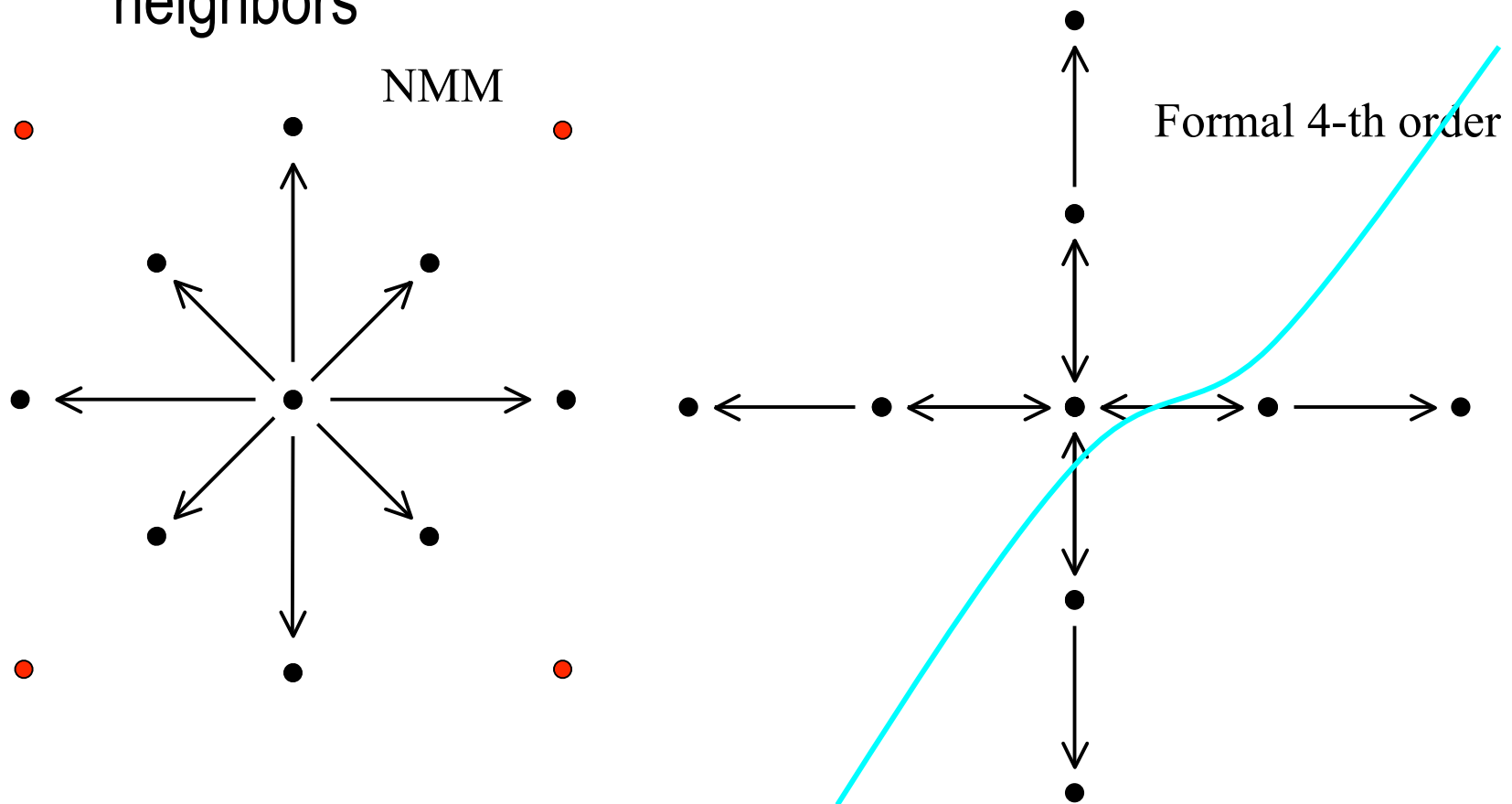


FIG. 9. The analogs of the eigenvalues of a finite difference Laplacian for a scheme which conserves E-grid energy and C-grid enstrophy. The values are nondimensionalized by multiplication by d^2 .

- Mass conserved
- In hydrostatic limit, advection of T conserves first and second moments
- Interchangeable flux/advection form in horizontal FD, mimetic differencing
- “Isotropized” horizontal divergence & advection operators on 9-point Arakawa Jacobian stencil

- Advection, divergence operators, each point talks to all neighbors



* E grid FD schemes also reformulated for, and used in ESMF compliant B grid model being developed

➤ Higher order formal accuracy?

- 4th order Janjic 1984 scheme already exists, Rancic (1988, MWR)
- Another sophisticated 4th order scheme recently tested
- Higher order of formal accuracy generally used **only for advection terms**, second order for gravity-inertia terms, **overall accuracy still second order**
- Higher order of formal accuracy not synonymous with higher accuracy; may be less accurate with noisy data!
- Extra computational boundary conditions required, generally more halo data to exchange (scaling) and more noise

- Problem, advection not clearly separable from “linear” terms beyond shallow water eqs

$$\frac{d\mathbf{v}}{dt} = -(1 + \varepsilon) \nabla_{\sigma} \Phi - \alpha \nabla_{\sigma} p + f \mathbf{k} \times \mathbf{v}$$

Second order
←

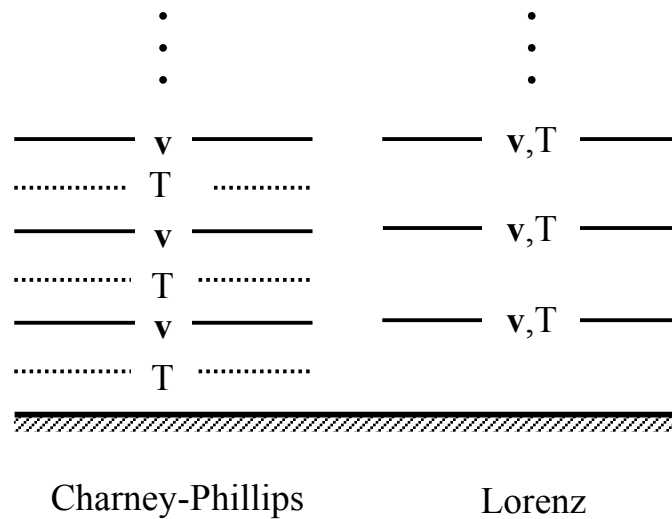
$$\frac{\partial T}{\partial t} = -\mathbf{v} \cdot \nabla_{\sigma} T - \dot{\sigma} \frac{\partial T}{\partial \sigma} + \frac{\alpha}{c_p} \left[\frac{\partial p}{\partial t} + \mathbf{v} \cdot \nabla_{\sigma} p + \dot{\sigma} \frac{\partial p}{\partial \sigma} \right]$$

- For consistency same order of accuracy in the omega-alpha term
- No visible benefit in practice

➤ Lateral boundaries

- Upstream advection in three rows next to the boundary
 - No computational outflow boundary condition for advection
- Enhanced damping along boundaries

➤ Vertical discretization



- Quadratic conservative vertical advection of u , v , T

➤ Time stepping

- **Explicit**, except for vertically propagating sound waves and vertical advection
- Different schemes for different processes:
 - Adams-Bashforth for horizontal advection of u , v , T and Coriolis force

$$\frac{y^{\tau+1} - y^{\tau}}{\Delta t} = \frac{3}{2} f(y^{\tau}) - \frac{1}{2} f(y^{\tau-1})$$

- Slight linear instability, can be tolerated in practice or stabilized by slight off-centering

- Crank-Nicholson for vertical advection of u , v , T

$$\frac{y^{\tau+1} - y^{\tau}}{\Delta t} = \frac{1}{2} [f(y^{\tau+1}) + f(y^{\tau})]$$

- Forward-Backward (Ames, 1968; Janjic and Wiin-Nielsen, 1977; Janjic 1979, Beitrage) for fast waves

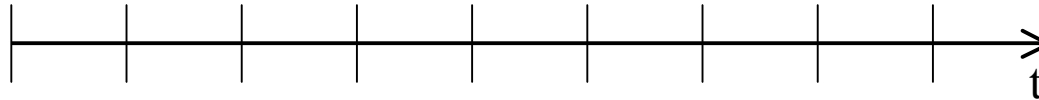
$$\frac{\partial u}{\partial t} = -g \frac{\partial h}{\partial x}, \quad \frac{\partial h}{\partial t} = -H \frac{\partial u}{\partial x}$$

$$h^{\tau+1} = h^{\tau} - \Delta t H \delta_x u^{\tau}, \quad u^{\tau+1} = u^{\tau} - \Delta t g \delta_x h^{\tau+1}$$

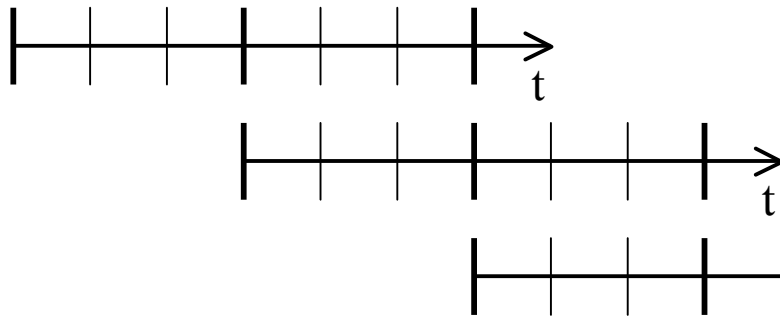
- Implicit for vertically propagating sound waves (Janjic et al., 2001; Janjic, 2003)

- No redundant computations, high comp. efficiency.

Janjic et al., 2001, MWR

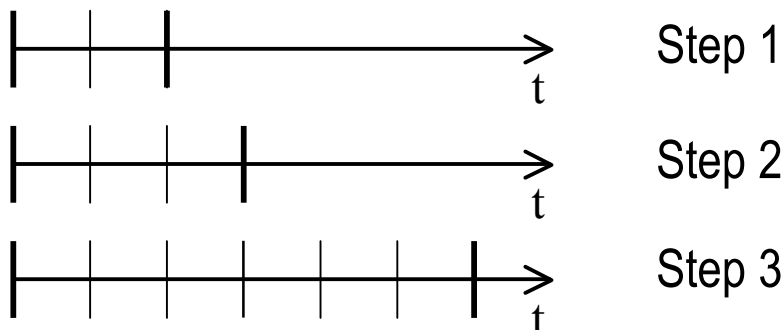


Klemp and Wilhelmson, 1978a, JAS



Each interval covered twice,
shorter small time steps on C grid.

Wicker and Skamarock, RK3, 2002, MWR



Each interval covered 1.8 times,
shorter small time steps on C grid.

➤ Passive substance advection

- Upstream, Lagrangian advection
- Gradient restoration by antialiasing
- Check for and elimination of new extrema, positive definite
- Forced conservation

➤ Dissipative processes

- Smagorinsky type nonlinear lateral diffusion (Janjic 1990, MWR), zeroed fluxes if the slope of coordinate surfaces exceed a critical value
- Horizontal divergence damping with enhanced damping of the external mode
- Coupling of elementary subgrids of semi-staggered grids (Janjic 1979, Contrib. Atmos. Phys.)

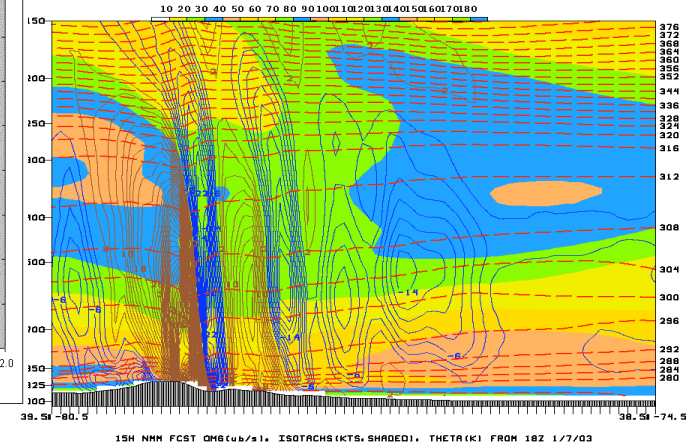
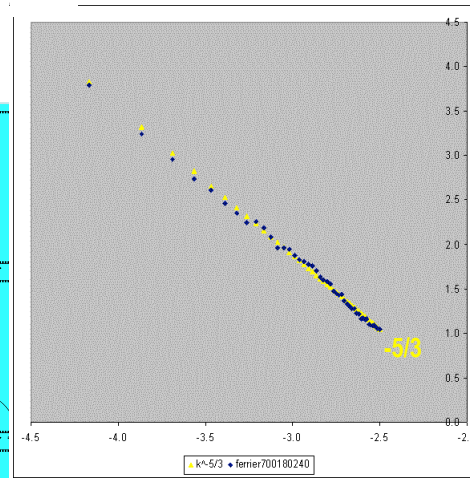
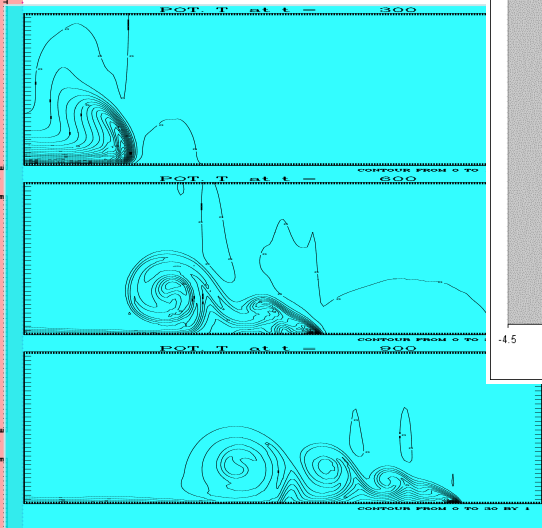
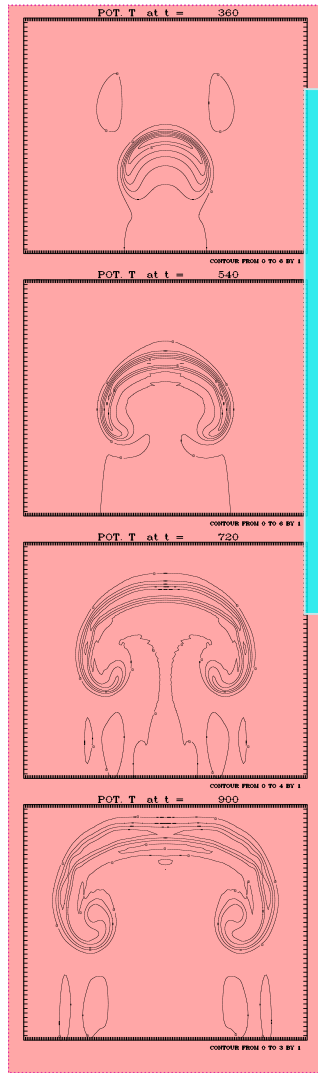
➤ Dynamics formulation tested on various scales

Warm bubble

Decaying 3D turbulence

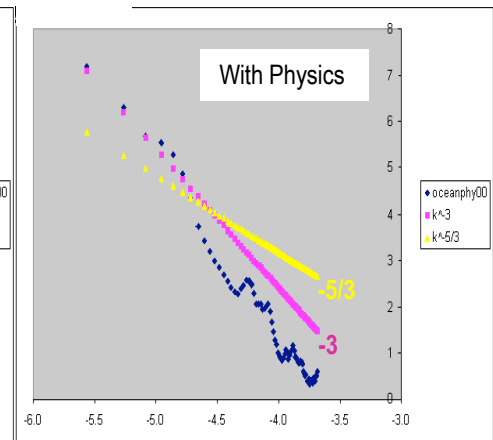
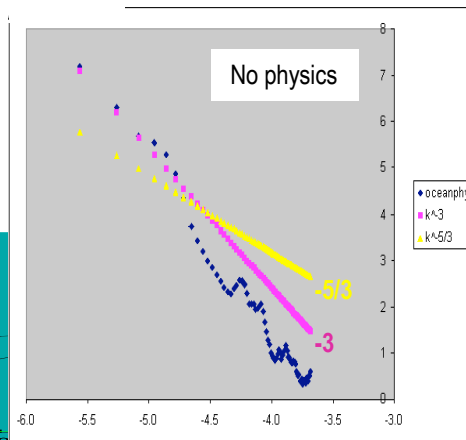
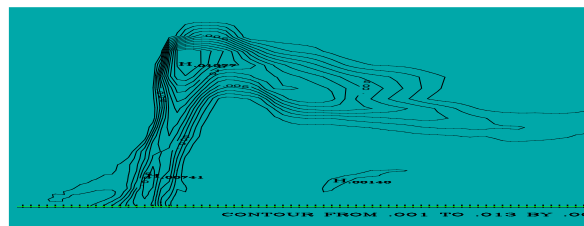
Cold bubble

Mountain waves



Atmospheric spectra

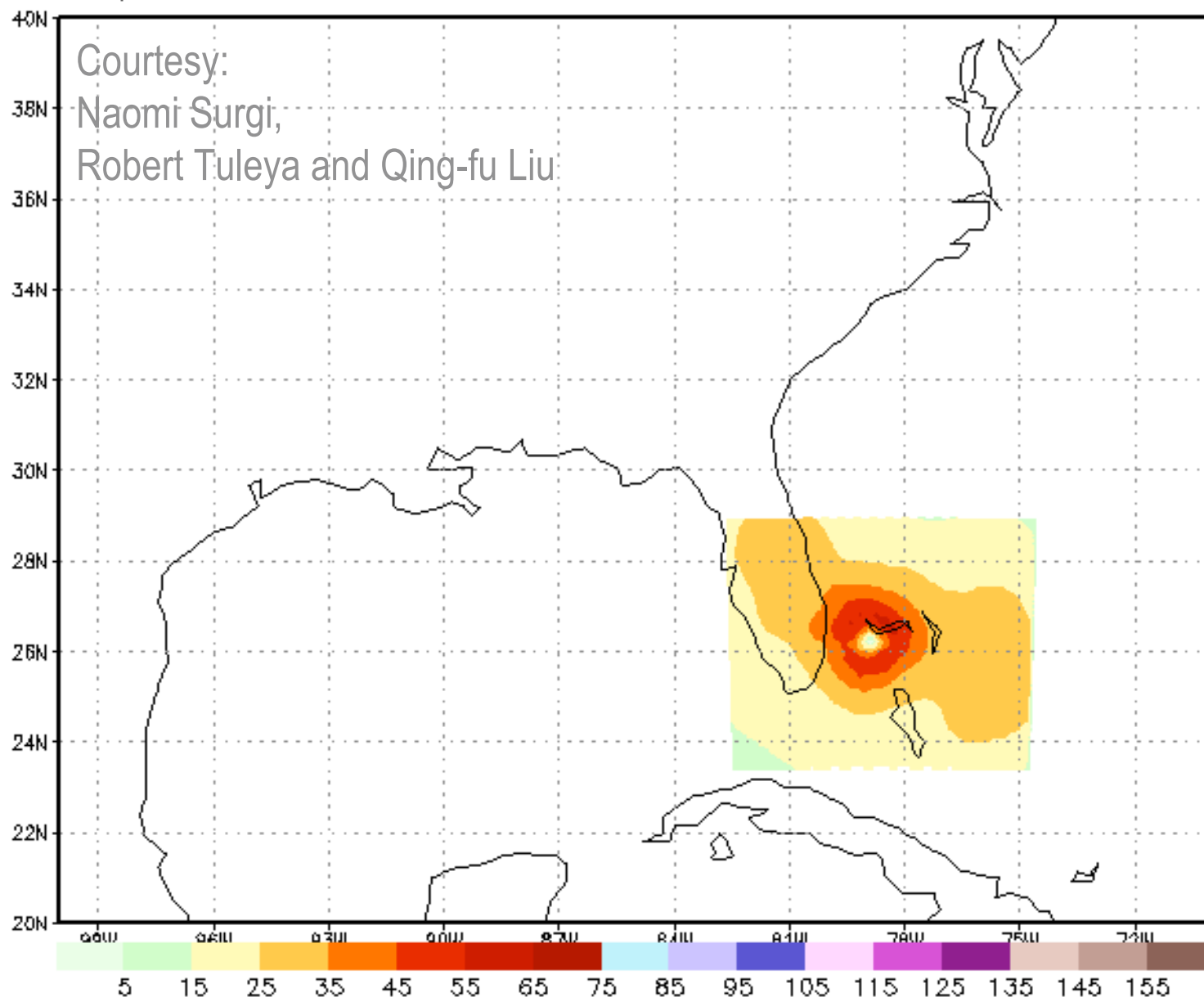
Convection



- Hurricane WRF-NMM (HWRF) (Naomi Surgi Program Leader)
 - Development began in 2002
 - Specific advanced physics
 - Multiple movable two-way interactive nesting
 - Nest movement following the center of the storm (Gopalakrishnan et al., 2002, MWR)
 - POM ocean model
 - Advanced data assimilation for hurricane core, ocean data assimilation
- First version in operations June 19th, 2007

AUG 25,2005 12Z:HURRICANE KATRINA – MOVING NEST FCST: 0

Courtesy:
Naomi Surgi,
Robert Tuleya and Qing-fu Liu



GrADS: COLA/IGES

Zavisa Janjic



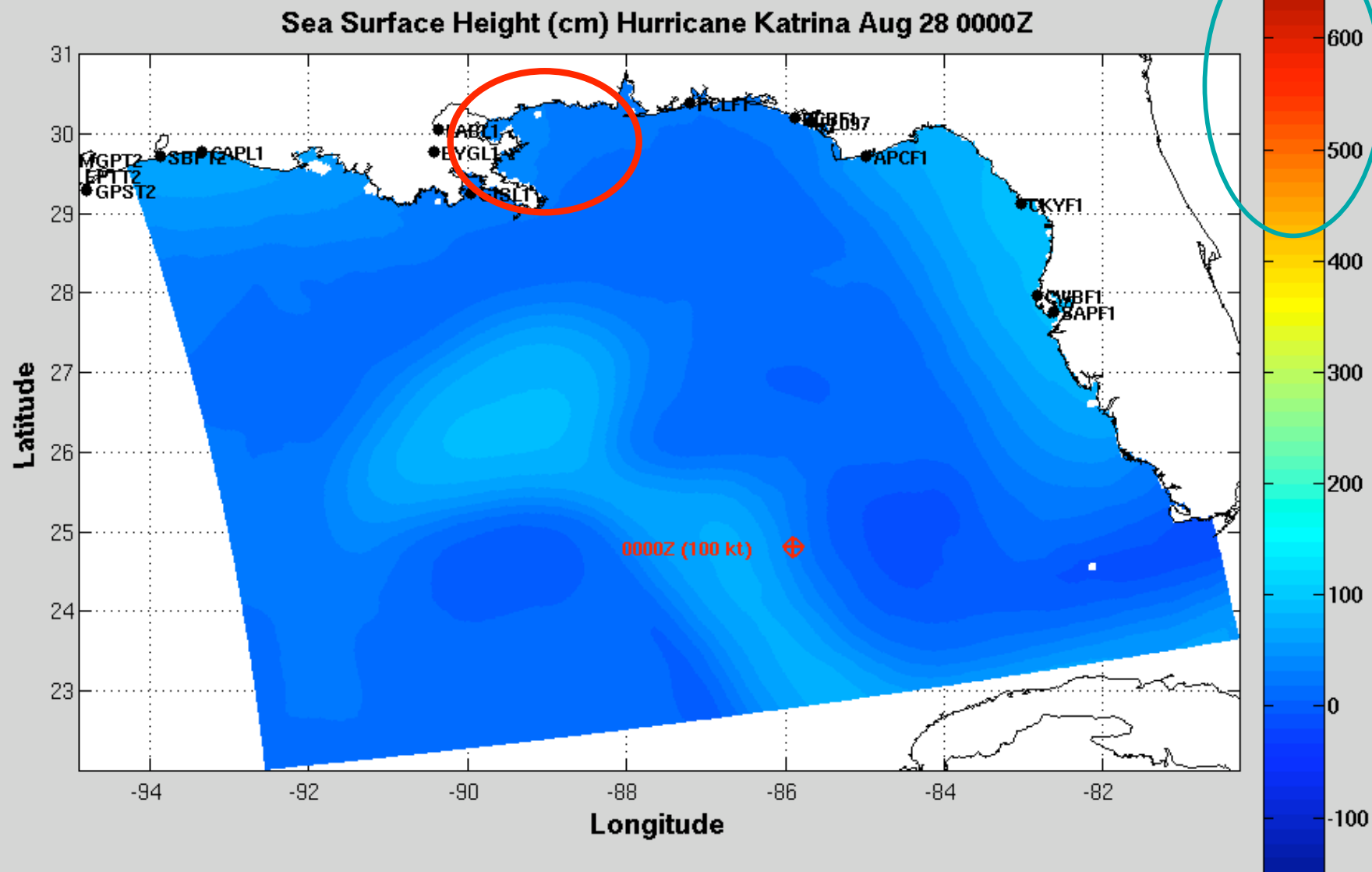
WRF NMM, July 2007

2005-12-19-23:53

57

HYCOM T&E Katrina

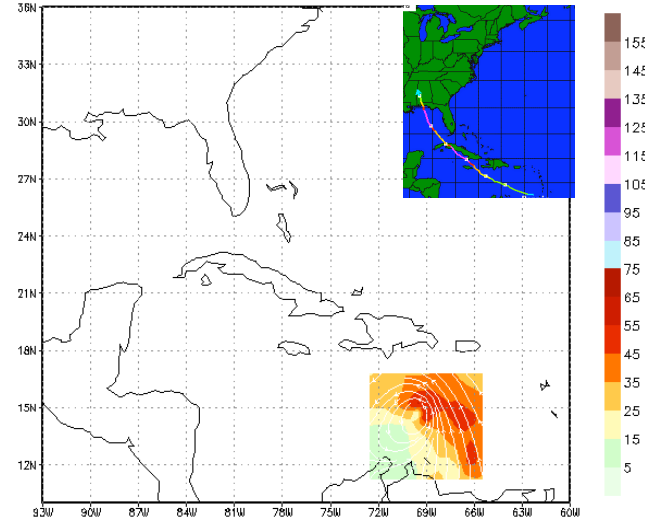
Courtesy: Naomi Surgi



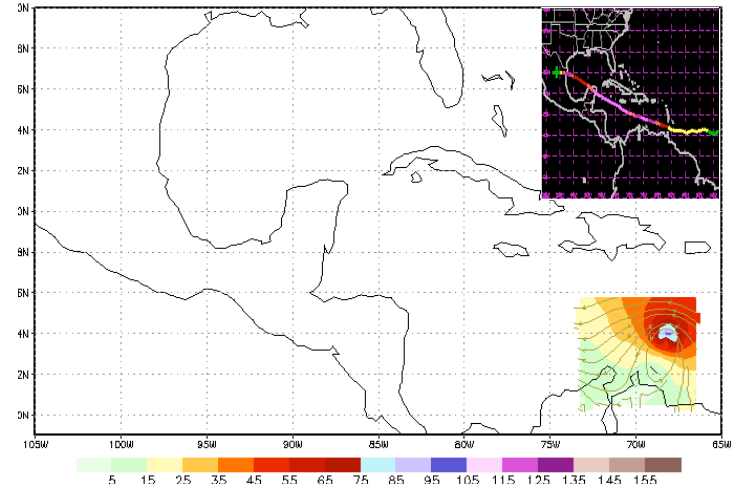
Five Day Forecasts with 2-Way Interactive Moving Nests

Courtesy:
Naomi Surgi,
Robert Tuleya and
Qing-fu Liu

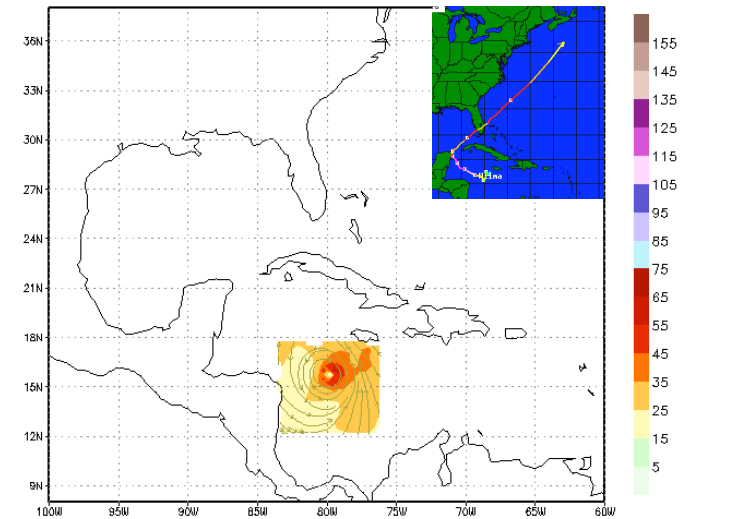
JULY 06, 2005 06Z: TS DENNIS MOVING NEST FCST: 0



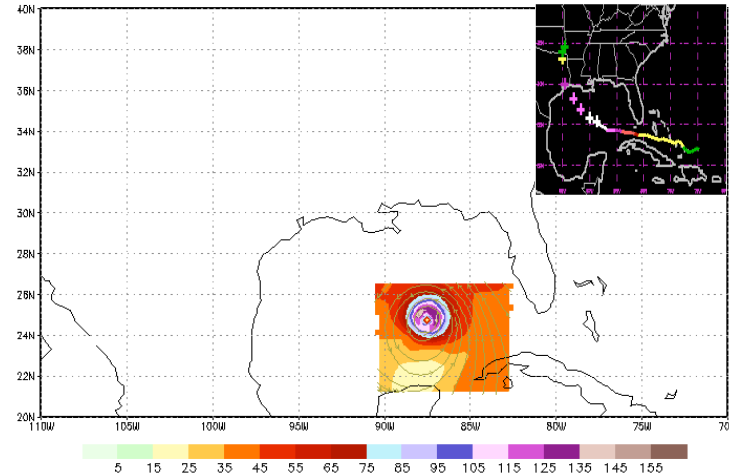
JULY 15, 2005 00Z: HURRICANE EMILY MOVING NEST FCST: 6



OCT 18, 2005 06Z: HURRICANE WILMA MOVING NEST FCST: 0



SEP 22, 2005 06Z: HURRICANE RITA MOVING NEST FCST: 0



GrADS: COL4/IGES

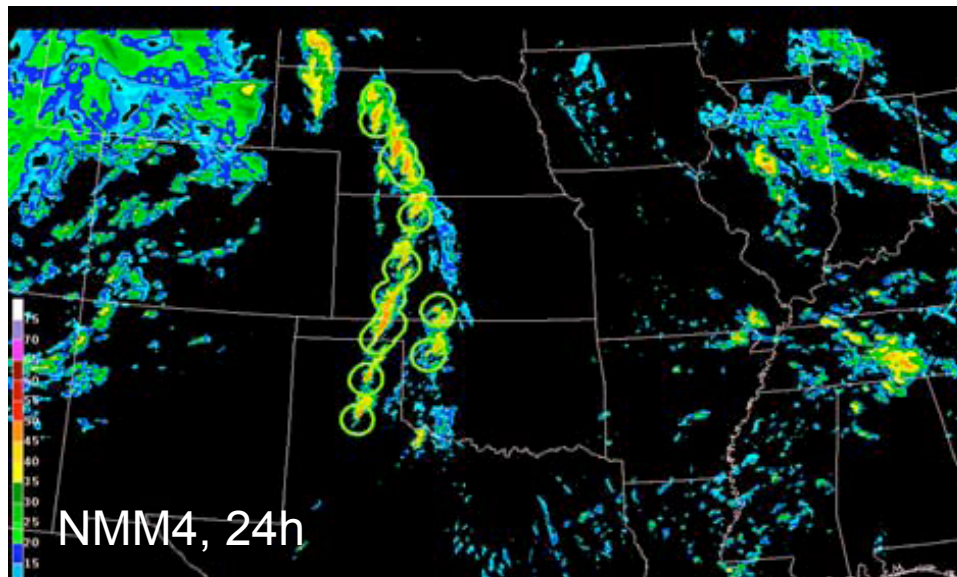
2005-09-22-0: GrADS: COL4/IGES

2005-10-18-10:54

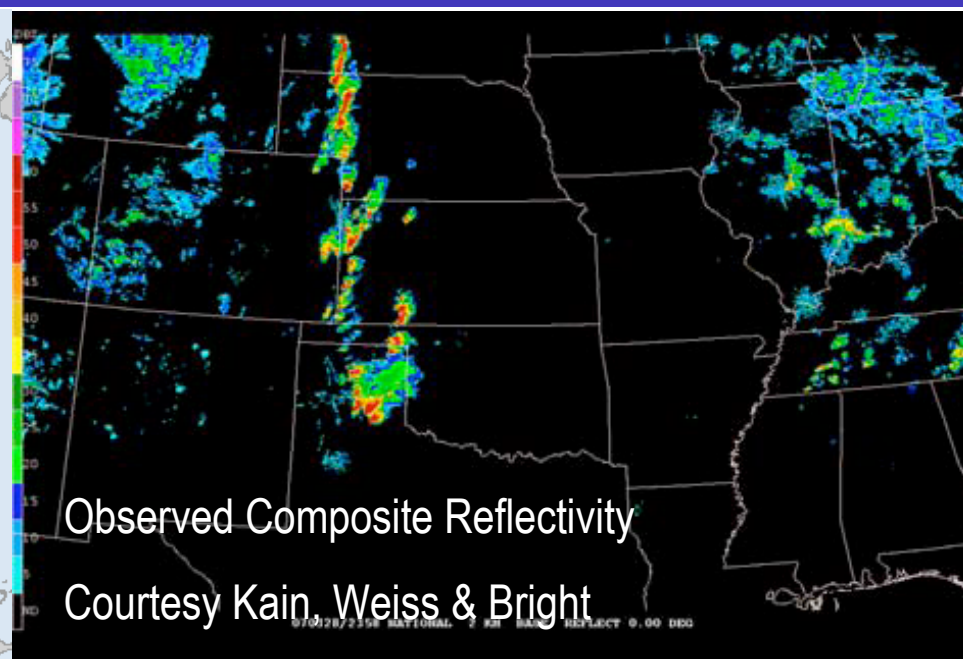
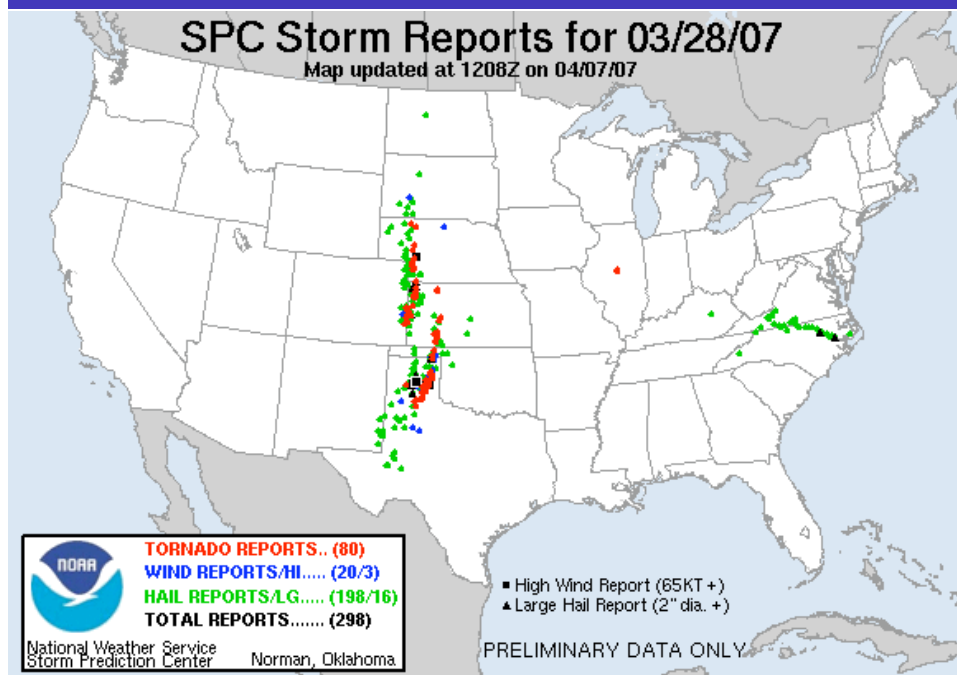
➤ National Severe Storm Laboratory (NSSL)/Storm Prediction Center (SPC) Spring Program 2004 (Weiss et al., 2004; Kain et al., 2005, WAF; ...).

- Carefully controlled assessment of potentials of experimental technologies for severe weather forecasting
- WRF-NMM, 4.5km, first time participation in 2004, run in support of SPC activities ever since

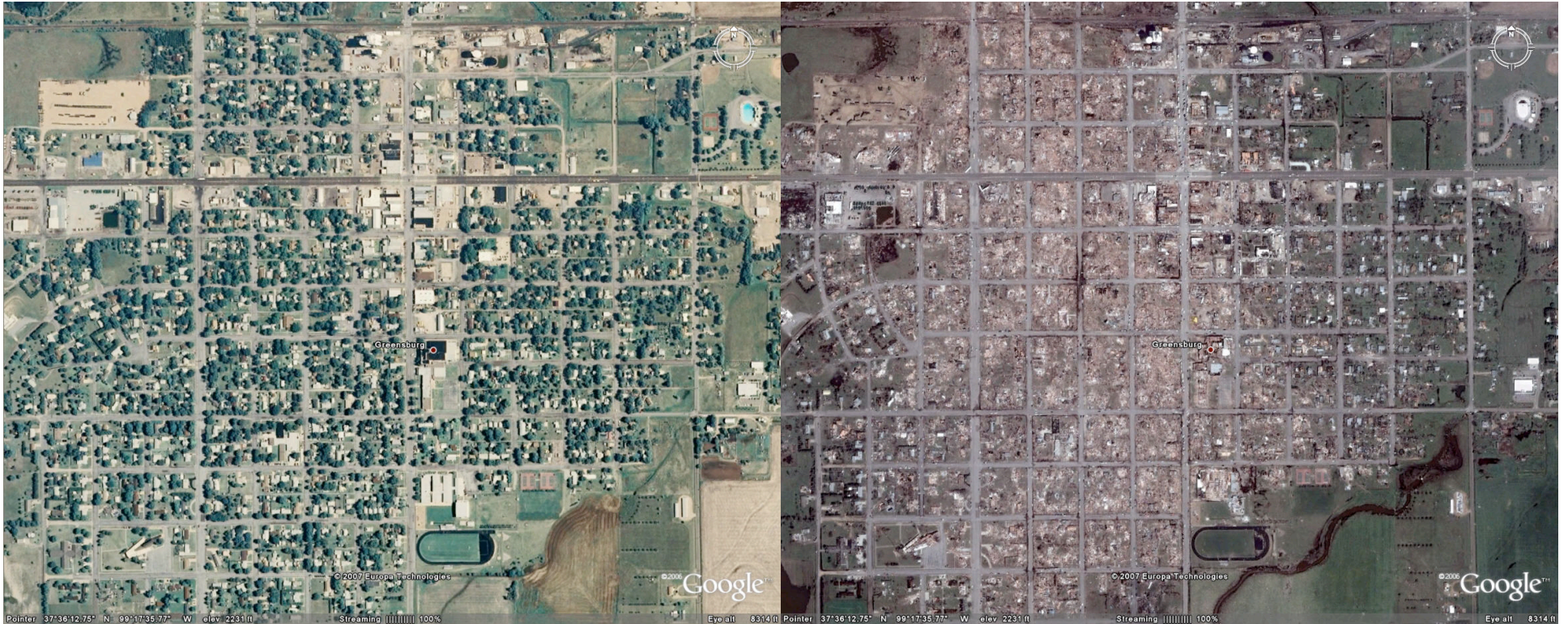
NOAA Hazardous Weather Testbed (Spring Program) 2007



24 hour forecasts, circles denote locations of rotating updrafts where updraft helicity is at least $50 \text{ m}^2\text{s}^{-2}$



➤ Greensburg, Kansas tornado



Before

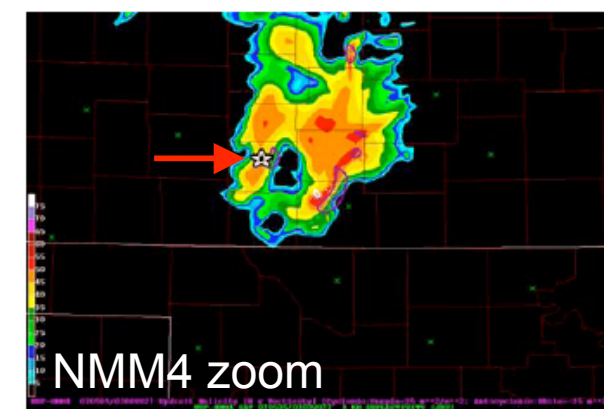
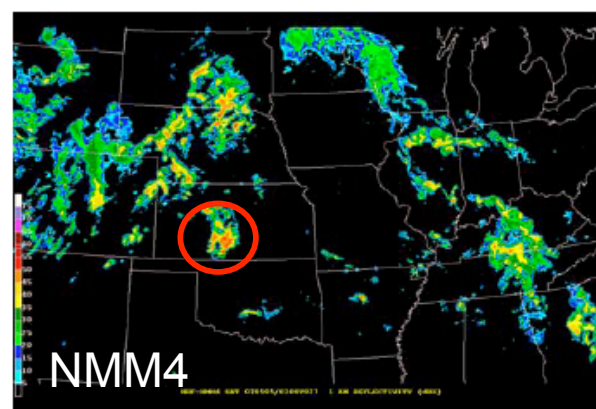
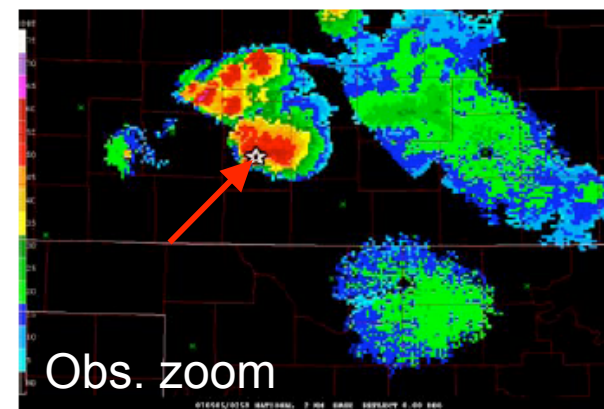
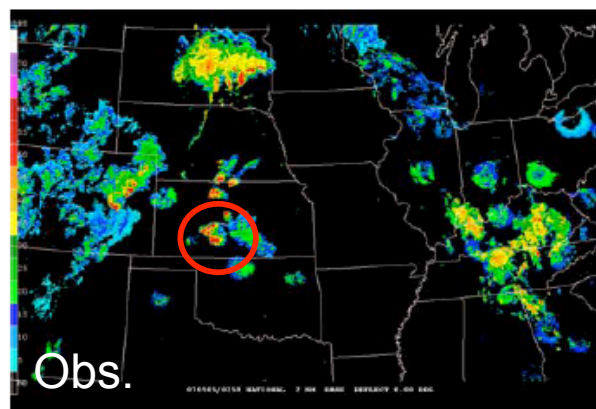
After

➤ Greensburg, Kansas, 27h forecast, reflectivity

THE NOAA HAZARDOUS WEATHER TESTBED:
COLLABORATIVE TESTING OF ENSEMBLE
AND
CONVECTION-ALLOWING WRF MODELS
AND SUBSEQUENT TRANSFER TO
OPERATIONS AT THE STORM PREDICTION
CENTER

Steven J. Weiss, John S. Kain, David R. Bright,
Jason J. Levit, Gregory W. Carbin,
Matthew E. Pyle, Zavisla I. Janjic, Brad S. Ferrier,
Jun Du, Morris L. Weisman, and Ming Xue

22nd Conference on Weather Analysis and
Forecasting/18th Conference on
Numerical
Weather Prediction, 2007 Park City, UT



Pyle Webpage Now Displaying Simulated Reflectivity

<http://www.emc.ncep.noaa.gov/mmb/mmbpll/cent4km/v2/>

**Simulated radar reflectivity,
lowest model level (dBZ)**

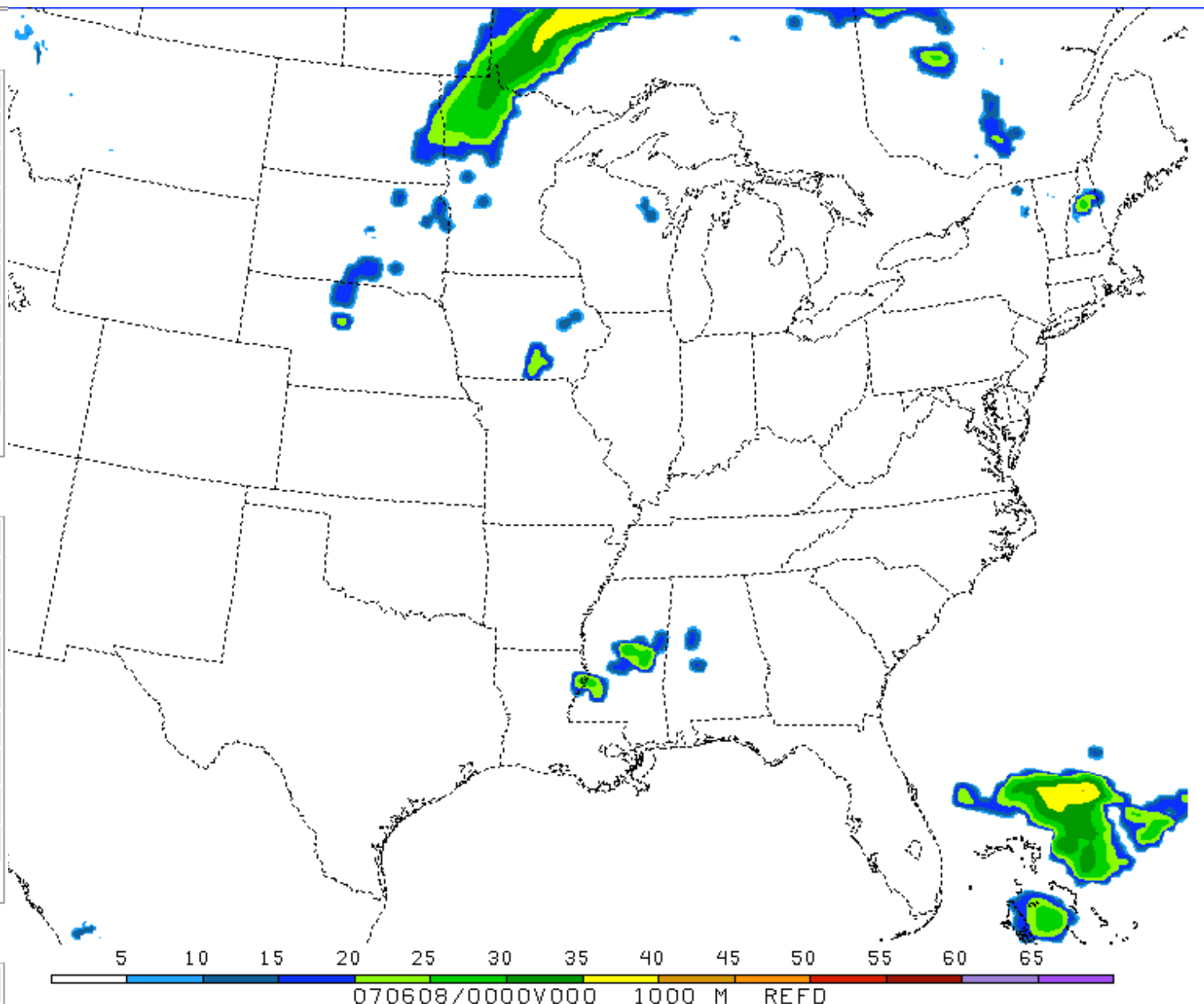
00h	01h	02h	03h
04h	05h	06h	07h
08h	09h	10h	11h
12h	13h	14h	15h
16h	17h	18h	19h
20h	21h	22h	23h
24h	25h	26h	27h
28h	29h	30h	31h
32h	33h	34h	35h
36h	NMM WRF Loop		

**Simulated radar reflectivity
(dBZ), 1000 m AGL**

00h	01h	02h	03h
04h	05h	06h	07h
08h	09h	10h	11h
12h	13h	14h	15h
16h	17h	18h	19h
20h	21h	22h	23h
24h	25h	26h	27h
28h	29h	30h	31h
32h	33h	34h	35h
36h	NMM WRF Loop		

**Simulated composite radar
reflectivity (dBZ)**

00h	01h	02h	03h
---------------------	---------------------	---------------------	---------------------



➤ Conclusions

- Robust, reliable, fast
- Atmospheric spectrum not due to computational noise
- NWP on near-cloud scales successful more frequently and with stronger signal than if only by chance
- Replaced the Eta as NAM at NCEP on June 20, 2006
- Near-cloud-scale runs at NCEP soon operational for severe weather forecasting
- Operational as hurricane WRF in 2007
- Operational and quasi-operational elsewhere (Europe, Canada)